

A risk-based multi-level stress test methodology: Application to six critical non-nuclear infrastructures in Europe

Sotirios A Argyroudis¹, Stavroula Fotopoulou¹, Stella Karafagka¹, Kyriazis Pitilakis¹, Jacopo Selva²,
Ernesto Salzano³, Anna Basco⁴, Helen Crowley⁵, Daniela Rodrigues⁵, José P. Matos⁶, Anton J. Schleiss⁶,
Wim Courage⁷, Johan Reinders⁷, Yin Cheng⁸, Sinan Akkar⁹, Eren Uckan⁹, Mustafa Erdik⁹, Domenico Giardini¹⁰, Arnaud
Mignan¹⁰

(1) Department of Civil Engineering, Aristotle University, Thessaloniki, Greece

(2) National Institute of Geophysics and Volcanology (INGV), Italy

(3) Department of Civil, Chemical, Environmental and Materials Engineering, University of Bologna, Italy

(4) AMRA, Italy

(5) EUCENTRE, Pavia, Italy

(6) Civil Engineering Institute, EPFL, Switzerland

(7) TNO, Netherlands

(8) School of Civil Engineering, Southwest Jiaotong University, China

(9) Bogazici University, Kandilli Observatory and Earthquake Research Institute, Turkey

(10) Department of Earth Sciences, Institute of Geophysics, ETH Zürich, Switzerland

Abstract

Recent natural disasters that seriously affected Critical Infrastructure (CI) with significant socio-economic losses and impact, revealed the need for the development of reliable methodologies for vulnerability and risk assessment. In this paper, a risk-based multi-level stress test method that has been recently proposed, aimed at enhancing procedures for evaluation of the risk of critical non-nuclear infrastructure systems against natural hazards, is specified and applied to six key representative CIs in Europe, exposed to variant hazards. The following CIs are considered: an oil refinery and petrochemical plant in Milazzo, Italy, a conceptual alpine earthfill dam in Switzerland, the Baku-Tiblisi-Ceyhan pipeline in Turkey, part of the Gasunie national gas storage and distribution network in the Netherlands, the port infrastructure of Thessaloniki, Greece, and an industrial district in the region of Tuscany, Italy. The six case studies are presented following the workflow of the stress test framework comprised of four phases: Pre-Assessment phase, Assessment phase, Decision phase and Report phase. First the goals, the method, the time frame, and the appropriate stress test level to apply are defined. Then, the stress test is performed at component and system levels and the outcomes are checked and compared to risk acceptance criteria. A stress test grade is assigned and the global outcome is determined by employing a grading system. Finally, critical components and events and risk mitigation strategies are formulated and reported to stakeholders and authorities.

36 **1. Introduction**

37 Critical infrastructure (CI) provides essential services to society and represents the backbone of economy, security
38 and health. Recent examples from key CIs have revealed that natural hazards can cause significant economic and
39 social damage, severely affect the provided services and lead to disasters, whilst cascading failures of CIs can
40 cause multi-infrastructure collapse and widespread consequences even in developed countries (Pescaroli and
41 Alexander 2016). Representative paradigms from Japan can be highlighted, i.e. the Tohoku earthquake, tsunami
42 and Fukushima nuclear release in 2011 (Krausmann and Cruz 2013) and the Hyogo-Ken Nanbu (Kobe)
43 earthquake in 1995 that caused extended damage to port and other critical infrastructure with long term
44 consequences (Chang 2000). Among past events in Europe, devastating flash floods in the spring of 2010 caused
45 extended dam failures in Poland (Reuters 2010), while major damage to industrial facilities was reported after the
46 2009 L'Aquila and 2012 Emilia earthquakes in Italy (Grimaz 2014).

47 The increase and intensity of such natural disasters over the last two decades (EMDAT 2019), which is correlated
48 to the ageing infrastructure and in some cases its inadequate design as well as to urban growth, climate change
49 and environmental degradation, has increased the interest of policy makers, practitioners and researchers toward
50 the understanding of infrastructure vulnerability and risk (Giannopoulos et al. 2012; Theocharidou and
51 Giannopoulos 2015; Opdyke et al. 2017). There is a remaining need to address gaps in existing knowledge in
52 order to better understand and assess the vulnerability and risk of CIs and improve their resilience against natural
53 hazards. In this respect, advanced and standardized tools for hazard and risk assessment of CIs are required, such
54 as the stress test tools , that include both low-probability high-consequences (LP-HC) events and so-called
55 extreme events, as well as the systematic application of these new tools to whole classes of critical infrastructure.
56 In particular, stress testing is the process of assessing the ability of a CI to maintain a certain level of functionality
57 under unfavorable conditions. Stress tests consider LP-HC events, which are not always accounted for in the risk
58 assessment procedures and tools, commonly adopted by public authorities or industrial stakeholders. They have
59 been initially developed for the financial and nuclear sectors, e.g. to check whether the safety and design
60 standards applied to nuclear power plants are sufficient to cover unexpected extreme events (Kutkov and
61 Tkachenko, 2017). In Europe, after the accident at the Fukushima nuclear power plant in Japan, a comprehensive
62 safety and risk assessment in the form of stress tests was performed on all nuclear plants (ENSREG 2012). Stress
63 tests contribute to the improvement of prevention and preparedness of critical infrastructure, providing the
64 roadmap for strengthening measures of the high-risk components and the improvement of emergency response
65 planning. Hence, stress tests contribute toward the resilience enhancement of the CIs, i.e. how they can adapt to
66 and recover from shocks.

67 In this context, an engineering risk-based multi-level stress test framework has recently been developed (Esposito
68 et al. 2016; 2019), aimed at enhancing the current procedures for evaluating the risk of critical non-nuclear
69 infrastructure against natural hazards, considering single or multi-hazards, probabilistic or scenario based

70 approaches, systemic analysis, interactions between components, cascading effects and an advanced grading
71 system.

72 The main objective of this paper is to demonstrate the applicability of this methodology, which is summarized in
73 Section 2, through six case studies of CIs in Europe exposed to different hazards: (1) an oil refinery and
74 petrochemical plant in Milazzo, Italy, by taking into account the impact of earthquakes and tsunamis (Section 3);
75 (2) a conceptual alpine earthfill dam in Switzerland under multi-hazard effects (Section 4); (3) the Baku-Tiblisi-
76 Ceyhan pipeline in Turkey, focusing on seismic threats at pipe-fault crossing locations (Section 5); (4) part of the
77 Gasunie national gas storage and distribution network in the Netherlands, exposed to earthquake and liquefaction
78 effects (Section 6); (5) the port infrastructures of Thessaloniki in Greece, subjected to seismic, tsunami and
79 liquefaction hazards (Section 7); and (6) an industrial district in the region of Tuscany, Italy, exposed to seismic
80 hazard (Section 8). These applications are representative of the following CI types: (i) single-site (case studies 1,
81 2 and 5), (ii) geographically extended (case studies 3 and 4), (iii) distributed multi-site (case study 6). The key
82 elements and output of the six applications are summarised in Section 9.

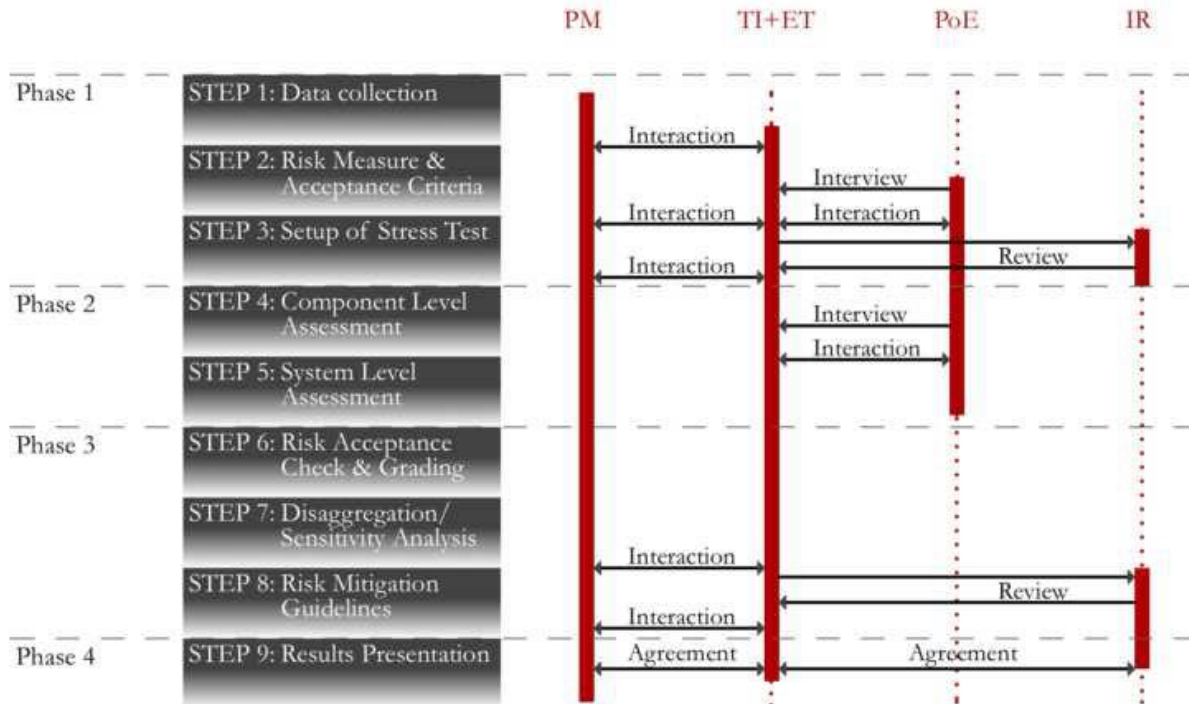
83

84 **2. Methodology**

85 **2.1 ST workflow and phases**

86 A harmonized framework for stress testing critical non-nuclear infrastructure systems has been recently proposed
87 (Esposito et al. 2019) aiming to quantify the safety and risk of individual components as well as of whole CI
88 system with respect to natural events and to compare the behavior of the CI to acceptable values. The multi-level
89 framework combines probabilistic and quantitative methods to characterise both extreme and common scenarios
90 and consequences, including potential multi-hazards and systemic amplification effects (e.g., Mignan et al. 2014;
91 2016a; 2016b). To manage subjectivity and uncertainty, the proposed framework includes a multiple-expert
92 integration (Selva et al. 2015), in which data, models and methods adopted for the risk assessment and the
93 associated uncertainty quantification are clearly documented and managed by different experts. Different roles
94 and responsibilities are assigned to different actors, namely the *project manager (PM)*, *technical integrator (TI)*,
95 *evaluation team (ET)*, *pool of experts (PoE)* and *internal reviewers (IR)*. Their roles and interactions are
96 illustrated in Figure 1, along with the workflow of the framework.

97



98
99 **Figure 1.** Workflow of the stress testing framework (Esposito et al. 2019)

100 The proposed framework is implemented in four main phases:

101 1. *Pre-Assessment Phase (steps 1 to 3):* the necessary data on the CI and hazards are collected. The risk measures
102 and acceptance criteria, the time frame, the most appropriate stress test level(s) and level of detail of the analysis
103 are defined depending on potential regulatory and stakeholder requirements as well as available resources and
104 data (Esposito et al. 2019).

105 2. *Assessment Phase (steps 4 to 5):* the stress test at component and system levels is performed following state-of-
106 the-art methods for the hazard, vulnerability and risk analysis.

107 3. *Decision Phase (steps 6 to 8):* the results of the Assessment phase are compared to the acceptance criteria that
108 have been defined in the Pre-Assessment Phase. This comparison results in a grade that informs about the degree
109 of the risk posed by the infrastructure, and, if the risk is unjustifiable or intolerable, how much the safety of the CI
110 should be improved until the next periodical verification. Critical events that most likely cause the exceedance of
111 a loss value of interest are identified through a disaggregation and/or sensitivity analysis. Risk mitigation
112 strategies and guidelines are formulated.

113 4. *Report Phase (step 9):* the experts present the stress test results to authorities and regulators of the CI. The
114 presentation includes the outcome of stress test in terms of the grade, the critical trigger events, the guidelines for
115 risk mitigation, and level of detail adopted in the stress test.

116 2.2 Stress test levels

117 Three *Stress Test Levels (ST-Ls)* are proposed. *Level 1 (ST-L1):* single-hazard component check (hazard-based,
118 design-based, risk-based); *Level 2 (ST-L2):* single-hazard system-wide risk assessment; *Level 3 (ST-L3):* multi-

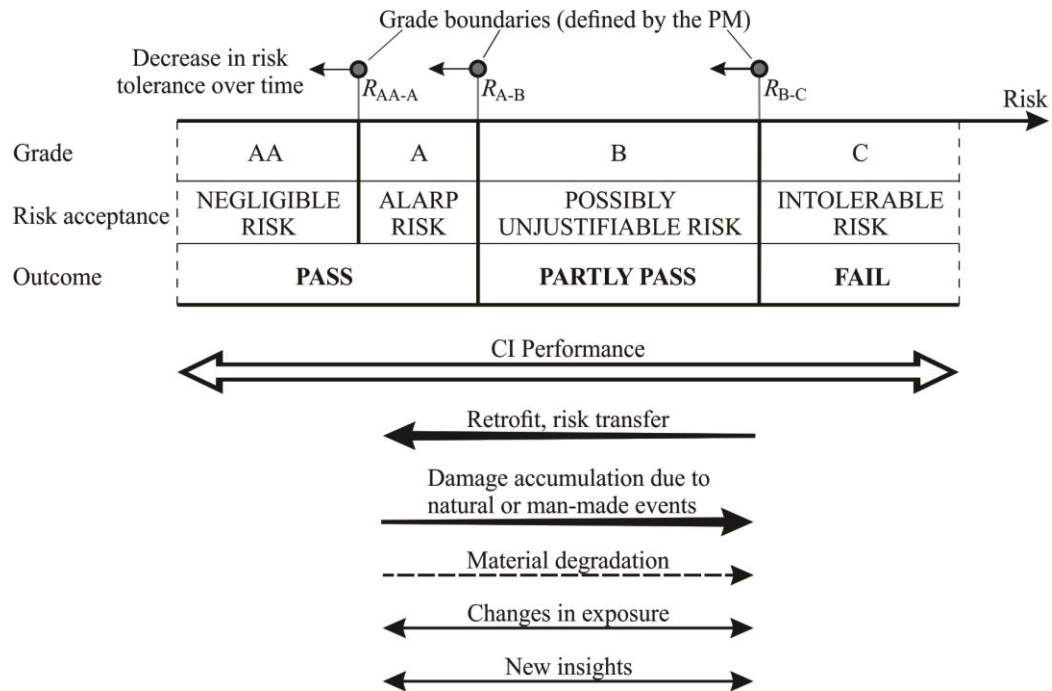
119 hazard system-wide risk assessment. Each level is characterized by a different scope (component or system) and
120 by a different complexity of the risk analysis. Within these three levels, potentially different implementations are
121 possible. The quantification of epistemic uncertainty may not be performed (sub-level a). If performed, it may be
122 based either on the evaluations of a single expert (sub-level b) or of multiple experts (sub-level c). In Levels ST-
123 L2 (sub-levels a, b and c) and ST-L3 (sub-levels a, b and c) probabilistic risk analysis (PRA) of the entire CI
124 (system) is performed. Complementary scenario-based analysis (sub-level d) may be performed for specific
125 conditions, events or hazards that cannot be included into the PRA due to methodological gaps. It is noted that
126 ST-L1 should be the routinely check for each CI and it might be deterministically (hazard or design-based) or/and
127 probabilistically (risk-based) defined.

128 **2.3 Penalty and grading system**

129 The stress test can result to three outcomes: *Pass*, *Partly Pass*, and *Fail* (Figure 2). In particular, the CI passes the
130 stress test if it attains grade AA or A. Grade AA corresponds to negligible risk and is expected to be the risk
131 objective for new CIs. Grade A corresponds to risk being as low as reasonably practicable (ALARP) (Helm, 1996;
132 Jonkman et al. 2003), and is expected to be the risk objective for existing CIs. The CI partly passes the stress test
133 if it gains grade B, which corresponds to the existence of possibly unjustifiable risk. The CI fails the stress test
134 when grade C is assigned, corresponding to the existence of intolerable risk. The boundaries between grades, i.e.
135 the risk acceptance criteria, are defined by the project manager of the stress test based on the requirements of the
136 regulators and societally acceptable risk norms. The form of the boundaries can be expressed using point
137 estimates, e.g. expected number of fatalities per year, or continuous functions, e.g. F-N curves, representing
138 cumulative frequency of the risk measure per given period of time. These boundaries may differ between
139 countries and industries. Further details can be found in Esposito et al. (2019).

140 The application of the stress test concepts to six CIs in Europe is summarized in the following sections. It is noted
141 that these applications include different ST levels based on the available data and resources in the framework of a
142 research study and they should not be considered as formal or complete stress tests. For a more elaborated
143 description of the case studies reference is made to Pitilakis et al. (2016).

144



145
146 **Figure 2.** Grading system for the outcome of stress test (Esposito et al. 2019)

147 **3. Application to oil refinery and petrochemical plant in Italy**

148 **3.1 Pre-Assessment phase**

149 Natural events may dramatically interact with industrial equipment with different intensity and hazards. Structural
150 failures may be indeed induced by seismic waves or tsunami waves, flooding and other combined scenarios.
151 Hence, industrial accidents may derive, such as fires, explosions, toxic dispersion or environmental disasters.
152 These scenarios are nowadays defined as Natech (Krausmann et al. 2011; Salzano et al. 2013; Renni et al. 2010;
153 Krausmann et al. 2016). Natech risks should be included in the industrial risk assessment (Quantitative Risk
154 Assessment, QRA), which is normally performed in early-design phase, during the licensing and land use
155 planning procedures, and other civil protection applications. Quite typically, results are given in terms of
156 locational risk and societal risks. The first is defined as the frequency per year that a hypothetical person will be
157 lethally affected by the consequences of possible accidents during an activity involving hazardous materials, e.g. a
158 chemical plant or transport activities. This risk indicator is a function of the distance between the exposed person
159 and the activity, regardless of whether people are actually living in the area, or at the specified location. Societal
160 risk is defined as the cumulative frequency that a minimum casualties due to possible accidents during an activity
161 with hazardous materials.

162 The refinery of Milazzo (Raffineria di Milazzo) is located in the north part of the island of Sicily, in Italy. It is an
163 industrial complex, which transforms crude oil into a series of oil products currently available on the market
164 (LPG, gasoline, jet fuel, diesel and fuel oil) and comprises a number of auxiliary services. The refinery has many

165 storage tanks containing a large variety of hydrocarbons, such as LPG, gasoline, gasoil, crude oil and atmospheric
 166 and vacuum residues. The capacities of the tanks vary from 100 m³ (fuel oil, gasoil, gasoline, kerosene) to 160
 167 000 m³ (crude oil). All tanks are located in catch basins (bunds) with concrete surfaces. The LPG is stored in
 168 pressurised spheres, while all other substances are stored in single containment tanks.

169 In the following, a Natech QRA for this installation, based on public information regarding the industrial process,
 170 has been performed.

171 3.2 Assessment phase

172 Probabilistic Hazard Analysis was performed for both tsunami and earthquake (ST-L2). For the tsunamis, we
 173 have focused only on tsunami of seismic origin, which is the dominant component in most areas of the world. The
 174 impact of natural hazards on the accident or release scenarios and frequencies is given in Table 1. These
 175 frequencies have been calculated by taking into account the methodology described in several previous works
 176 (Salzano et al. 2015; Basco and Salzano 2016), where equipment vulnerability with respect to the intensity of the
 177 natural events has been assessed by taking into account the construction characteristics of equipment and, more
 178 important, the new limit states based on the release of content.

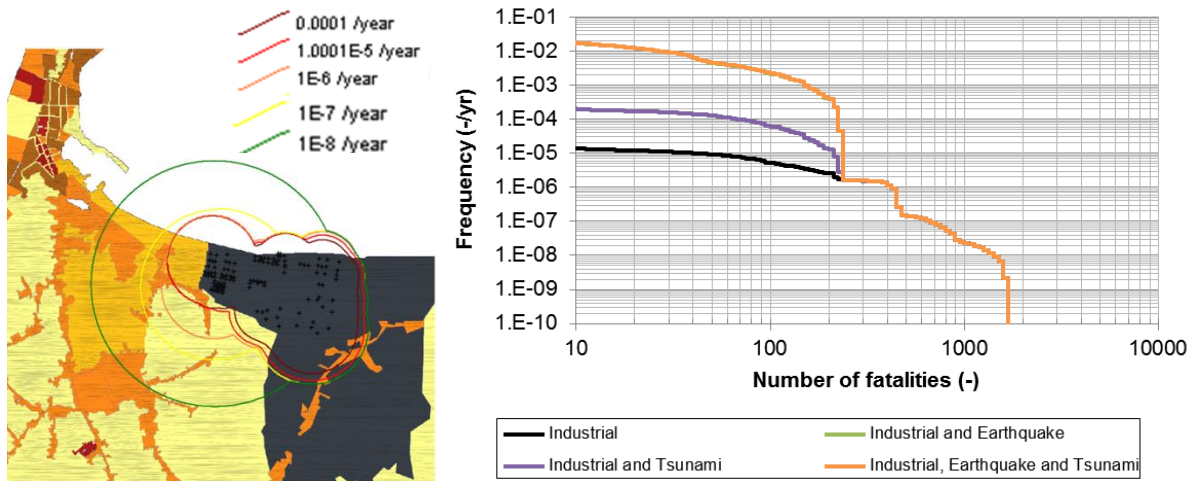
179 **Table 1.** Scenarios and frequencies for stationary vessels due to natural hazards

Scenario	Frequency (-/yr)		
	<i>Atmospheric vessels</i>	<i>Pressurized vessels</i>	<i>Pipelines</i>
Earthquake			
Instantaneous release of the complete inventory	$3.70 \cdot 10^{-3}$	$1.16 \cdot 10^{-9}$	-
Continuous release of the complete inventory in 10 min at a constant rate of release	$3.70 \cdot 10^{-3}$	$1.16 \cdot 10^{-9}$	-
Continuous release from a hole with an effective diameter of 10 mm	$7.33 \cdot 10^{-2}$	0	-
Full bore rupture	-	-	$5.56 \cdot 10^{-2}$
Tsunami	<i>Atmospheric vessels</i>	<i>Pressurized vessels</i>	<i>Pipelines</i>
Instantaneous release of the complete inventory	$1.85 \cdot 10^{-5} - 3.47 \cdot 10^{-4}$	0	-
Continuous release of the complete inventory in 10 min at a constant rate of release	$1.85 \cdot 10^{-5} - 3.47 \cdot 10^{-4}$	0	-
Continuous release from a hole with an effective diameter of 10 mm	0	0	-
Full bore rupture	-	-	0
Earthquake + Tsunami			
Instantaneous release of the complete inventory	$3.7 \cdot 10^{-3} - 4.05 \cdot 10^{-3}$	$1.16 \cdot 10^{-9}$	-
Continuous release of the complete inventory in 10 min at a constant rate of release	$3.7 \cdot 10^{-3} - 4.05 \cdot 10^{-3}$	$1.16 \cdot 10^{-9}$	-
Continuous release from a hole with an effective diameter of 10 mm	$7.33 \cdot 10^{-2}$	0	-
Full bore rupture	-	-	$5.56 \cdot 10^{-2}$

180

181 **3.3 Decision phase**

182 Results obtained for the Natech QRA for the refinery of Milazzo, in terms of locational risk and societal risk is
183 presented in Figure 3. The isorisk curves take into account the combination of all natural and industrial hazards.
184 The right part of the same figure allows the evaluation of the contribution of either industrial or natural events,
185 separately, and their relative weights. The fact that the curves for Industrial and Earthquake and Industrial,
186 Earthquake and Tsunami coincide, means that tsunami adds a negligible contribution to risk. This methodology
187 can be then used for the decision phase, in terms of licensing, land use planning, civil protection plan (emergency
188 plan), early design and industrial and environmental authorizations.



189 **Figure 3.** Locational risk (left) and societal risk (right) – Hazard combinations (industrial, seismic, tsunami)

190
191
192

193 **3.4 Report phase**

194 Naturally induced hazards can play an important role in the total risk associated with the presence of installations
195 with dangerous goods. For the specific site analyzed, our stress testing results indicate that the predicted tsunamis
196 can only damage a limited number of the atmospheric storage vessels along the shoreline. Hence the increase on
197 the total risk is limited. Nonetheless, the overloading of emergency response should be considered, at least for the
198 tanks along the coastline.

199 Of more importance is the effect of an earthquake, which significantly increases the failure frequency of
200 atmospheric storage tanks. Therefore, reinforcing the emergency response for multiple fire scenarios would be
201 beneficial, together with structural improvement of the tanks. Neither an earthquake nor a tsunami significantly
202 increases the failure frequency of, and hence risk imposed by, pressurized vessels (like LPG spheres). As for the
203 considered site, the risk is largely dominated by the LPG tanks when failing due to industrial-related causes,
204 whereas the impact of the natural hazards is limited. All in all though, naturally induced hazards should be
205 considered when determining the overall risk and the risks associated with natural disaster. The communication

206 among key actors (emergency responders, public authorities, industrial stakeholders) is deemed mandatory,
207 according to the Seveso directive (EC 2012). In particular, the communication should be improved by re-thinking
208 of the information to the population related to the industrial risks, which is still mandatory by the Seveso directive
209 (EC 2012), but completely lacking for the natural-technological interaction.

210 **4. Application to a large dam in Switzerland**

211 Dams operate by storing water (and its potential energy) in their reservoirs and releasing it when convenient.
212 Often, that potential energy can produce massive damages if not controlled adequately. In the event of a failure or
213 breach a large amount of water travels downstream in the form of a dam-break wave, affecting downstream areas
214 more seriously than natural floods. To fully understand the risks associated with large dams one should therefore
215 take into account the dam, the reservoir, the downstream areas, and the multiple elements and interactions that
216 characterize what can be called the dam-reservoir system.

217 Dam safety is most commonly tested using deterministic frameworks where the system's response is simulated
218 and analyzed in detail for a given number of limit cases (Zenz and Goldgruber 2013; Gunn et al. 2016). Although
219 proven very successful, the deterministic approach's focus on limit cases leaves countless possibly disastrous
220 combinations of events unchecked. Furthermore, the probability of occurrence of the limit cases under test is not
221 necessarily known and, therefore, even if the risk associated with the infrastructure can qualitatively be inferred to
222 be small when the test succeeds, it remains unknown in quantitative terms. This justifies further investments on
223 probabilistic alternatives.

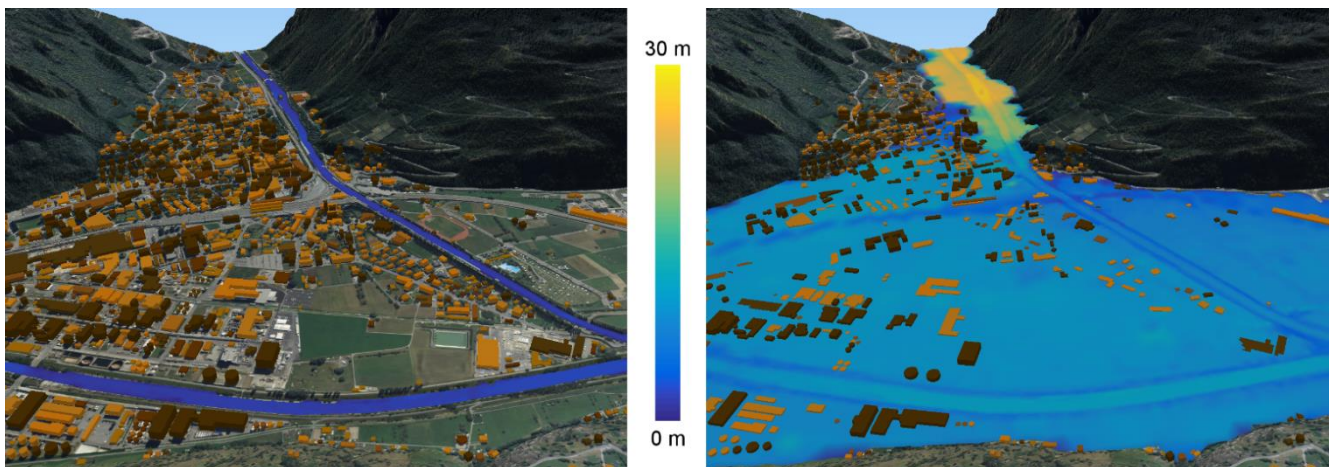
224 The present application aimed to develop a flexible probabilistic framework that separates the risk assessment for
225 large dams in two sequential steps: the analysis of the dam-reservoir system, that provides information about the
226 frequency of failures and the conditions under which water is released; and the downstream areas, where the
227 progression of each dam-break wave is accounted for and damages are evaluated. The modeled system includes a
228 dynamical representation of the dam-reservoir system that relies on the Generic Multi-Risk (GenMR) framework
229 (Mignan et al. 2014; 2016) and accounts for multiple hazards, multiple elements, and a large number of non-linear
230 influences and feedbacks between them. Also included in the system is a module capable of efficiently predicting
231 inundation parameters for each simulated dam failure case to roughly 30 km downstream, where a sizable urban
232 agglomeration is assumed to exist (Figure 4).

233 A large conceptual alpine earthfill dam was taken as a case study. The infrastructure is approximately 100 m high,
234 with a reservoir capable of holding over 100 000 000 m³ of water. It is equipped with a spillway in order to cope
235 with excessive water levels, a bottom outlet that allows for the control of the volume of water stored, and a
236 hydropower system through which the main purpose of the dam is fulfilled, i.e. producing energy.

237 **4.1 Pre-Assessment phase**

238 The considered hazards included earthquakes, floods, internal erosion, and electromechanical malfunctions in key
239 systems. Regarding elements, the dam and foundation, the bottom outlet, the hydropower system, the spillway,
240 and the reservoir were modeled. The most relevant interactions considered were the damages induced on
241 elements, the damage states that lead to changes in operations, the probability of internal erosion events and how
242 it is affected by reservoir levels and damage through overtopping. Focusing on the downstream area, the response
243 of each building to the inundation was also modeled resorting to fragility curves. Hazards were defined according
244 to statistical distributions and, for each case, epistemic uncertainty on the parameters of those distributions was
245 assumed. The response of each element to relevant hazards was also defined probabilistically, according to
246 fragility functions.

247 The objectives of the stress test were two-fold. First, regarding the frequency of failures. Second, the expected
248 damages downstream as a direct consequence of such failures. Risk measures were, accordingly, the expected
249 return period of dam failure events and the expected built volume downstream of the dam that would be destroyed
250 as a result.



251 **Figure 4.** Illustration of the impact of a specific dam-break wave on an urban area downstream

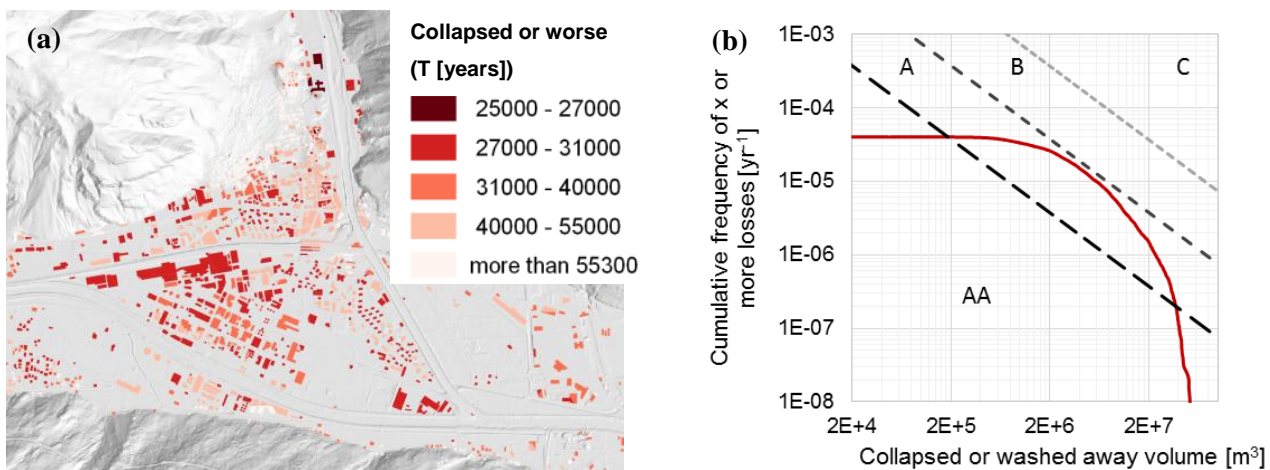
252 **4.2 Assessment phase**

254 The backbone of the assessment phase is the component level assessment (ST-L1). Here, as the case study is
255 conceptual, it was admitted that all the elements of the system comply to and slightly exceed regulatory
256 requirements. The ST-L2 system level assessment for a single hazard (earthquake) was undertaken in both
257 deterministic and probabilistic models. In the ST-L3 system level assessment, for multiple hazards, the full
258 integration of the dam-reservoir and downstream analysis realms was made. Through the simulation of 20 000
259 000 years of dam operation a number of failures with different characteristics was sampled. It should be clear that
260 the simulations are not extended 20 000 000 years into the future; rather, it is different possibilities for “next” year
261 that are simulated. The number of simulations should be large enough to sample events of the order of magnitude
262 of the return period intended for the infrastructure. For example, in 20 000 000 simulations it can be expected to

263 find, on average, 2 000 events with a return period of 10 000 years or above. For each one of these, inundations
 264 parameters were estimated throughout the downstream valley. Computations were performed by a machine
 265 learning meta-model trained based on detailed 2D hydraulic simulations of representative dam-break events.
 266 Integrating the information from all the simulations, including aleatoric and epistemic uncertainty, it was possible
 267 to gain remarkable insight on the system. Figure 5a, for example, illustrates the return period of individual
 268 buildings collapsing or being washed away as a result of dam failures.

269 4.3 Decision phase

270 With a return period of 25 000 years for failures, the conceptual dam was shown to meet the first of three risk
 271 objectives by having, on average, less than one failure per 10 000 years. In what concerns damages in the
 272 downstream area, the goal was to limit expected damages to the loss of one household per 100 years. In concrete
 273 terms, this was assumed to be equivalent to an average built volume loss of 7.5 m^3 per year due to dam failures.
 274 After integrating expected losses in the downstream area, however, a substantially higher value of 200 m^3 of built
 275 volume lost per year was estimated. As a consequence, the second risk objective was not met. Despite this the
 276 expected losses were deemed acceptable as the undesirably high value is more a product of the number of
 277 households exposed to the dam-break wave than on the frequency of dam failures, being therefore and to some
 278 extent beyond the influence of changes that the dam may undergo. The third objective is bound to the analysis of
 279 a F-N curve (Figure 5b), in this case prepared to show the cumulative frequency of built volume collapsing or
 280 being washed away as a consequence of a dam break upstream. The threshold AA-A corresponds to a risk of 7.5
 281 m^3/yr , the A-B threshold, corresponding to the third risk objective, to $75 \text{ m}^3/\text{yr}$, and finally B-C to $750 \text{ m}^3/\text{yr}$
 282 (roughly equivalent to a household per year).



283
 284 **Figure 5.** Illustration of results from the study on large dams. a) return periods of individual buildings being collapsed or
 285 washed away following a dam failure upstream. b) F-N curve based on collapsed or washed away built volume following a
 286 dam failure upstream (adapted from Pitilakis et al. 2016)

287 **4.4 Report phase**

288 The flexibility of the GenMR framework (e.g., Mignan et al. 2014), particularly when combined with machine
289 learning methods that allow extraordinary gains in computational performance, makes this inclusive and formally
290 correct estimate of risk attainable. Obviously, this is a highly desirable feature when performing a stress test.

291 From the three objectives established in this stress test, one, concerning the dam-reservoir system and the
292 probability of failures taking place, was met with a failure return period of 25 000 years, safely above the 10 000
293 years mark. The second, focusing on the expected losses downstream, was not. Quantitatively the chosen risk
294 metric was more than 25 times over the objective of 7.5 m³/year of built infrastructure collapsed or washed away.
295 The third objective, defined on the basis on an F-N curve, classified the risk as ALARP.

296 In this conceptual case, earthquakes appear to be responsible for the most part of the expected losses. They have a
297 direct impact on the dam but can also lead to the catastrophic elevation of water in the reservoir through damages
298 to the outlet structures. Investing in a more resilient bottom outlet would virtually prevent all overtopping events,
299 being perhaps the most direct and cost-effective way to reduce risk. Regarding the downstream losses, a possible
300 use of the analysis results and maps is to reinforce, provide with shelters or relocate the buildings which are
301 assessed as high risk. However, the risk downstream is not only dependent on the probability of failure of the
302 dam-reservoir system, but also on the amount of people and infrastructure exposed at risk. Once the CI is
303 considered safe, it may be more cost-effective to invest on the protection of the downstream area than on the dam
304 itself (for example, providing better warning systems and escape routes). For the conceptual CI that was studied,
305 some potential failures could be averted by drawing down the reservoir. Therefore, beyond the notions of fragility
306 that were explored, the resilience of the dam-reservoir system beyond the design requirements is very much
307 defined by the capacity to perform a successful and timely drawdown operation. Cascade effects become
308 important when the possibility of drawing down the reservoir is lost, and a substantial inflow arrives.

309 Concluding, to evaluate the risk associated with the failure of a large dam it is important to bring together a
310 number of experts in different fields, relevant to the structure itself, the foundation and hydrology. For an accurate
311 quantification of impacts downstream it is essential to collect data and knowledge on infrastructure, property and
312 populations, including the evacuation in case of a failure. Compared to other CIs, the verification of the safety of
313 large dams is quite developed as these infrastructures are built not to fail. An improvement of existing approaches
314 is the consideration of uncertainty, in the quantification of hazards and fragility.

315

316 **5. Application to major hydrocarbon pipeline in Turkey**

317 The hydrocarbon pipelines usually extend over very long distances by crossing borders, hard geographic
318 conditions and geo-hazard areas. As of seismic effects, they are prone to permanent fault displacement (PFD)
319 hazard because fault crossings (upon their rupture) may cause large deformations on the hydrocarbon pipelines

320 and impose a major risk for their structural integrity. When such pipelines are exposed to PFD, typical damage is
 321 in the form of local buckling due to axial compression and/or bending (in normal burial depths) and global
 322 (beam) buckling (in shallow burial depths) or in submarine pipelines. The rupture of the pipe could be due to
 323 severe compressive buckling of the pipe wall or tensile fracture.

324 This section implements the stress testing methodology for seismic risk assessment of pipeline failure due to PFD.
 325 The Baku-Tiblisi-Ceyhan (BTC) pipeline is used as the case study that crosses several strike-slip fault segments
 326 in the Eastern Anatolia Fault.

327 **5.1 Pre-Assessment phase**

328 The diameter and thickness of the pipes at the five main fault segments are 42 inches (1.0688 m) and 20.62 mm,
 329 respectively. The pipeline trench is trapezoidal-shaped and packed with loose-to-medium granular cohesionless
 330 backfill with minimum soil cover. The pipeline crosses five fault segments along Eastern and North Anatolia
 331 Fault zones with fault-pipe crossing angles varying between 30° and 90°. All other compiled data information
 332 about the mechanical features of BTC pipeline as well as fault properties important in PFD computations are
 333 given in Pitilakis et al. (2016).

334 The risk measure in this case study is the pipeline rupture or loss of pressure integrity due to fault offsets. Table 2
 335 lists the probability ranges of different risk tolerances according to the grading system of the stress test
 336 methodology.

337 **Table 2.** The risk tolerance levels and the probabilities defined for the stress test grade

Grade	AA	A	B	C
Risk tolerance	Negligible	ALARP	Possibly Unjustifiable risk	Intolerable
Probability range in 2475-year return periods	0%-2%	2%-10%	10%-50%	50%- 100%
CI performance	pass		partly pass	fail

338
 339 Eidinger and Avila (1999) propose four performance classes (life safety, key operational, other operational and
 340 disruption) to represent severity of pipe failure at pipe-fault crossings. These four performance goals are set to
 341 four pipeline failure probabilities (Table 2) that are defined as 1% (life safety), 2% (key operational), 10% (other
 342 operational) and 50% (disruption) against PFD underground-motions represented by 2475-year return period
 343 uniform hazard spectral ordinates.

344 The stress tests comprise of three steps at component level (ST-L1), performing hazard-based (moderate
 345 accuracy), design-based (advanced accuracy) and risk-based assessment (high accuracy).

346 **5.2 Assessment phase**

347 **5.2.1 Hazard-based assessment:** the 2475-year PFDs (recommended by ALA 2001; 2005) at five pipe-fault
 348 crossings are computed from the Monte-Carlo based probabilistic PFD hazard (Chen and Akkar, 2017; third row
 349 in Table 3). They are compared with the prescribed ALA hazard requirements (second row in Table 3). The
 350 comparisons indicate that of the five pipe-fault crossings, the computed 2475-year PFD hazard at #2, #3 and #4
 351 pipe-fault crossings are larger than the ALA requirements (last row in Table 3). The potential impact of mega-
 352 ruptures in the region (Mignan et al., 2015) was not included in this analysis, since the mechanism of mega
 353 ruptures is complicated and models to estimate the fault displacement are yet to be proposed.

354 **Table 3.** Hazard-based assessment – comparison of 2475-year return period PFD hazard with ALA requirements

	Pipe-fault crossings				
	#1	#2	#3	#4	#5
2475-year ALA2001 (design)	1.31m	1.18m	1.61m	3.84m	0.63m
2475-year ALA2001 (assessment)	0.73m	2.25m	3.91m	4.49m	0.44m
Compliance (design \geq assessment)	yes	no	no	no	yes

355
 356 **5.2.2 Design-based assessment:** The tensile pipe strain under the 2475-year PFD is compared with the allowable
 357 tensile pipeline strain provided in ALA (2001). The allowable tensile pipe strain is designated as 3% in these
 358 design provisions. The comparisons are done for all five pipe-fault crossings and the tensile strains at these pipe-
 359 fault crossings comply with the code requirements (Table 4).

360 **Table 4.** Calculated tensile strains at the designated fault offsets

Pipe-fault crossing	Crossing angle	2475-year fault offset (m)	Tensile strain	Compliance ($\leq 3\%$)
#1	60°	0.73	0.33%	Yes
#2	70°	2.25	0.85%	Yes
#3	30°	3.91	2.18%	Yes
#4	45°	4.49	2.00%	Yes
#5	90°	0.44	0.18%	Yes

361
 362 **5.2.3 Risk-based assessment:** The annual exceedance rate of pipeline failure is compared with the suggested
 363 allowable pipeline failure rates in the literature. The probabilistic pipeline failure is achieved by integrating the
 364 probabilistic fault displacement hazard, mechanical response of pipe due to fault displacement and empirical pipe
 365 fragility function (Cheng and Akkar 2017). The aggregated effects of tensile and compressive strains developed
 366 along the pipe are considered in the seismic pipe failure risk. The annual failure probability (P_f) for pipelines at
 367 fault crossings is computed for different pipe-fault crossing angles (α) by considering the uncertainty in α . The

368 inaccuracy in fault-pipe crossing angle is modeled by a truncated normal probability with alternative standard
 369 deviations of 2.5° and 5°.

370 The acceptable annual pipe failure rate of $4.0 \cdot 10^{-5}$ (Honegger and Wijewickreme 2013) is compared with the pipe
 371 failure rates at five designated pipe-fault crossings (Table 5). The comparisons indicate that pipe-fault crossings
 372 #3 and #4 are critical as their computed failure rates are larger than the allowable annual failure rate. The listed
 373 annual failure rates are also used to compute the aggregated failure risk along the whole BTC pipeline to complete
 374 the probabilistic risk assessment. Two marginal probabilities are computed: (a) perfect correlation between pipe
 375 failures at the five pipe-fault crossings (P_{fc}) and (b) independent pipe failures at the five pipe-fault crossings (P_{fi}).
 376 The aggregated marginal failure probabilities are very high and they range between 40% and 50% (Table 6) that
 377 fall into grade B: possibly unjustifiable risk according to Table 2.

378 **Table 5.** Comparisons of annual pipe failure exceedance rates with the allowable pipe failure rate

Pipe-fault crossings	σ (standard deviation) : Uncertainty to pipe-fault crossing angles (α)			Compliance ($\leq 4.0 \cdot 10^{-5}$)
	0	2.5	5	
#1	$3.142 \cdot 10^{-6}$	$3.183 \cdot 10^{-6}$	$3.304 \cdot 10^{-6}$	Yes
#2	$1.833 \cdot 10^{-6}$	$2.256 \cdot 10^{-6}$	$3.293 \cdot 10^{-6}$	Yes
#3	$1.967 \cdot 10^{-4}$	$1.964 \cdot 10^{-4}$	$1.955 \cdot 10^{-4}$	No
#4	$5.987 \cdot 10^{-5}$	$5.981 \cdot 10^{-5}$	$5.962 \cdot 10^{-5}$	No
#5	$1.973 \cdot 10^{-5}$	-	-	Yes

379
 380 **Table 6.** Aggregated failure probabilities of BTC pipeline under 2475-year PFD hazard before and after the risk mitigation
 381 strategies

	P_{fc} (perfectly correlated case)	P_{fi} (statistically independent case)
Before retrofit	38.56 %	51.0 %
After retrofit	0.775 %	2.206 %

382
 383 **5.3 Decision and Report phase**

384 The probabilistic pipe failure risk assessment yields higher probabilities of pipe failure at #3 and #4
 385 pipe-fault crossings. Therefore, these pipeline segments are identified as critical components and it is
 386 decided to be upgraded.

387 The effective retrofitting of the pipeline segments at the critical crossings is to change the pipe-fault intersection
 388 angle. When the intersection angles of these three pipe-fault intersection angles are changed to $\sim 80^\circ$, the resulting
 389 aggregated risk probability is reduced to negligible levels

390 Table 6). The disaggregation and sensitivity analysis of BTC pipe failure assessment bring forward the higher
391 PFD hazard and small pipe-fault crossing angles (resulting in higher tensile strain) as the main sources of large
392 failure probabilities at the pipe-fault crossings #3 and #4.

393 **6. Application to gas storage and distribution network in Netherlands**

394 This section summarizes the application of the stress test methodology to part of the main gas distribution
395 network of Gasunie Gas Transport Services (Gasunie-GTS). The Groningen field is a large natural gas field
396 located in the northern Netherlands, contributing to approximately half of the natural gas production in the
397 country. The gas distribution relies on a major gas pipeline infrastructure, with a total length of over 12 000 km of
398 installed pipes in. Located in an area of very low tectonic seismicity, gas extraction in the region has led to an
399 increase in seismicity since the early 1990s. A sub-network (Figure 6) is studied located in the induced earthquake
400 prone area, directly above the main gas field covering an area of approximately 3360 km².

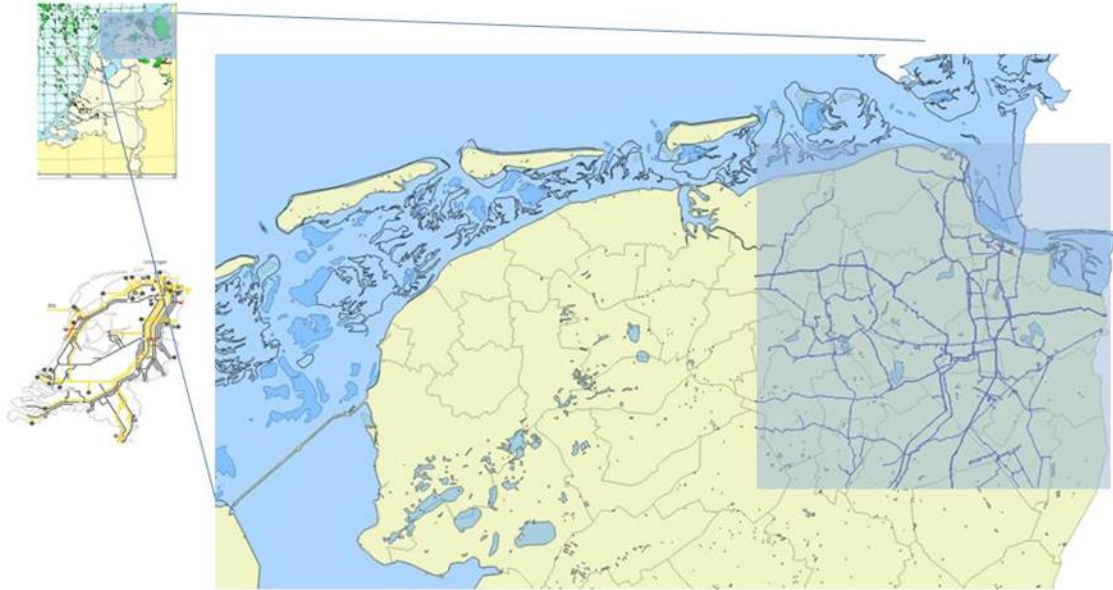
401 **6.1 Pre-Assessment phase**

402 Numerous seismic hazard studies dedicated to the Groningen area have been performed over the past several
403 years and are still ongoing. In the current stress test one of the earlier model versions was adopted: the so-called
404 Z1 model from Dost et al. (2013) for the seismic zonation (four zones), the Akkar et al. (2014a; 2014b) modified
405 ground motion model (Bommer 2013) and the classical Gutenberg-Richter (GR) relation (Gutenberg and Richter
406 1956). A maximum magnitude (for the stress test only) value of 6.0 was applied and the annual event rate for
407 events with $M \geq 1.5$ is set to 30 events per year (Dost et al. 2013).

408 Serviceability Ratio (SR) and Connectivity Loss (CL) are used as risk measures (Esposito et al. 2015). The
409 Serviceability Ratio is directly related to the number of demand nodes in the network, which remain accessible
410 from at least one source node following an earthquake. Connectivity Loss measures the average reduction in the
411 ability of demand nodes to receive flow from source nodes due to an earthquake event.

412 An as low as reasonable practicable (ALARP) grade of the risk measures is targeted for the existing gas transport
413 network to pass the stress test (Jonkman et al. 2003). In the Netherlands a standard for quantified risk assessment
414 (QRA) exists, issued by the national “Committee for the Prevention of Disasters” (CPR 18E 1999). In the current
415 application of the stress test methodology to the Gasunie-GTS case, no full QRA was performed for the 1000 km
416 sub-network. However, values for the annual failure rates originally prescribed in (CPR 18E 1999) and adjusted
417 values nowadays used for the Gasunie network are selected to define grade boundaries (Table 7):

418



419

420

Figure 6. Selected sub system of the gas distribution network (right) located above main natural gas field (top left)

421

Table 7. Definition of grading boundaries for the gas network

Boundary	Pipe [$\text{yr}^{-1}\text{km}^{-1}$]	Station [yr^{-1}]
AA-A	$8 \cdot 10^{-6}$	$8 \cdot 10^{-6}$
A-B	$6 \cdot 10^{-5}$	$6 \cdot 10^{-5}$
B-C	$1.4 \cdot 10^{-4}$	$1.4 \cdot 10^{-4}$

422

423

For illustrative purposes only, indicative grading boundaries are attributed to the values of the performance parameter connectivity loss (CL). The boundaries used are taken from (Esposito et al. 2016). No actual calibrations for these bounds with respect to economic loss or fatalities exist yet for the sub-network at hand and the grading is indicative and provisional.

427

The stress test has been performed up to ST-L2 considering earthquake as single hazard and conducting a full Probabilistic Risk Analysis using Monte Carlo simulations for the network analysis. ST-L1 considers individual components for which also a risk based approach is applied. As the methods in this case for ST-L1 and ST-L2 are both Monte Carlo based, ST-L1 makes use of the ST-L2 results.

431

Accuracy levels targeted are classified as advanced: the stress test is risk based for the network as well as for the individual components with site specific hazard analyses, structure specific fragility functions and using outcomes of dedicated studies by, among others, the NAM, KNMI, TNO and Deltares as well as by an international community of experts (WINN_TA-NAM 2016).

435

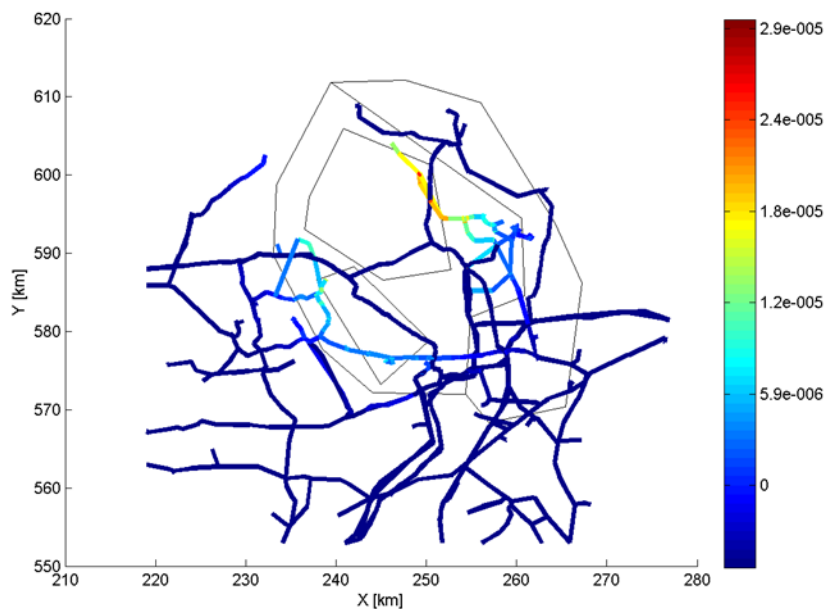
6.2 Assessment phase

436

The ST-L2 for the evaluation of the seismic network performance is consisted of five major steps:

- 437 • Seismic hazard assessment of the region considering gas depletion as source of the seismic activities.
- 438 • Evaluation of ground motion hazard in terms of PGA, PGV and permanent ground displacement (due to
- 439 liquefaction).
- 440 • Seismic demand evaluation at each station and pipe section to obtain the failure using fragility curves.
- 441 • Vulnerability analysis through the use of a connectivity algorithm to assess the network performance.
- 442 • Probabilistic risk assessment in terms of mean network functionality and annual exceedance curves.

443 The likelihood of liquefaction given the soil conditions in the Groningen area, the Netherlands, was first assessed
 444 (Miraglia et al. 2015) in which a model based on the Idriss-Boulanger model (Idriss and Boulanger 2008) is used.
 445 Two soil profiles based on CPT tests were analyzed by describing the soil properties as stochastic parameters and
 446 sampling the liquefaction response of the layers with earthquake events. Sampling results were then summarized
 447 as fragility curves as a function of PGA values for the two soil profiles. Soil liquefaction can cause permanent soil
 448 displacements as well as floating or sinking of pipe segments due to gravity. Structural reliability calculations are
 449 performed for distinct pipe configurations and probabilities of failure are calculated conditional on liquefied soil.
 450 For transient load effects, again structural reliability calculations are performed based on Newmark’s formulae of
 451 seismic strain for buried pipelines (Newmark and Rosenblueth 1971). As a result transient load fragility curves
 452 were obtained as function of PGV values. For the stations, a generic fragility curve from the HAZUS
 453 methodology (NIBS 2004) was adopted.



454 **Figure 7.** ST-L1: annual failure frequencies (per km) for the pipe sections (black lines on background indicate the earthquake
 455 zones)
 456

457 Seismicity, network and network properties are modeled with the OOFIMS (Franchin et al. 2011) tool and Monte
458 Carlo simulations are performed. The results show a good performance with respect to CL (Figure 8): the annual
459 probability of having a connectivity loss of e.g. 50% or more is $3.6 \cdot 10^{-5}$. For the serviceability ratio very high
460 exceedance frequencies for all values of the serviceability ratio are found, with only a drop near SR reaching one.
461 Hence the results show a high robustness of the network, indicating a vast redundancy in possible paths between
462 demand and source nodes. Sampled results (failure, no failure) per component (pipes/stations) from the ST-L2
463 Monte Carlo analysis of the network are used to calculate ST-L1 annual failure probabilities per component (e.g.
464 Figure 7). Pipes as well as stations showed satisfactory performance in terms of reliability.

465 **6.3 Decision phase**

466 With respect to the grading on component level the following results are obtained:

- 467 • Pipe sections: Most pipe sections obtain grade AA, some obtain grade A. The pipe sections pass the stress
468 test.
- 469 • Stations: Most stations are classified with grade AA or A. Some, near or within the seismic zone, obtain
470 grade B. The stations partly pass the stress test.

471 With respect to the network performance Figure 8 presents the values for the connectivity loss relative to the
472 indicative grading boundaries. The network performance is shown to comply with grade AA and passes the stress
473 test.

474 These findings are obtained despite a number of conservative assumptions made with respect to fragilities. Also
475 the seismic demand was modeled in a conservative way with e.g. a maximum magnitude of 6 and an annual rate
476 of occurrence for $M_L > 1.5$ equal to 30. Reducing these assumptions to a maximum magnitude of 5 and or an
477 annual rate equal to 23 leads to all stations complying with grade AA or A.

478 With respect to components, both types (pipe sections and stations) are found to contribute evenly to the network
479 performance. From these:

- 480 • Specific pipe sections can to some extent be identified as being a weakest link in the network. These
481 sections should be checked on their current actual state assessing the need for upgrading.
- 482 • For the stations a rather strong assumption is made with respect to the fragility curve adopted. These
483 should be quantified in more detail and depending to findings retrofitting of stations might be necessary.

484 In the current analysis soil liquefaction is the dominant failure mechanism. As much uncertainty still exists in the
485 liquefaction fragilities for the Groningen area, further studies into these fragilities and their geographical
486 distribution is recommended.

487 **6.4 Report phase**

488 The stress test is performed as being initiated by the asset owner, the Gasunie Transportservices and as such
 489 reported to the asset owner. No formal presentation of the outcome of the stress test to (other) CI authorities
 490 and/or regulators is foreseen. Reporting, in terms of the grade, the critical events, the guidelines for risk
 491 mitigation, and the accuracy of the methods adopted in the stress test is accomplished in Pitilakis et al. (2016).

492 Most pipe sections and stations conform to grade AA or A, except for few stations that reach grade B. Turning
 493 points are magnitude $M_L=5$ or annual rate $N_{M>1.6}=23$ at which all components comply to grade AA or A and pass
 494 the stress test, see Table 8.

495 At the time of performing the stress test, no governing earthquake specific design requirements existed in the
 496 Netherlands. The CI's safety and resilience will be improved by reassessing the need for retrofitting of a confined
 497 number of pipe sections identified. The stress test also revealed the need for site-specific fragility functions for the
 498 Gasunie-GTS stations as well as further research into the liquefaction mechanisms for the Groningen site
 499 conditions.

500 **Table 8.** Stress test results for Gasunie-GTS sub-network

Item	M_{max}	$N_{M>1.6}$	Grading	Result
Pipe sections	6	30	AA, A	Pass
Stations	6	30	AA, A, B	Partly pass
	5	30	AA, A	Pass
	6	23	AA, A	Pass
Network <i>CL</i>	6	30	AA, A	Pass

501

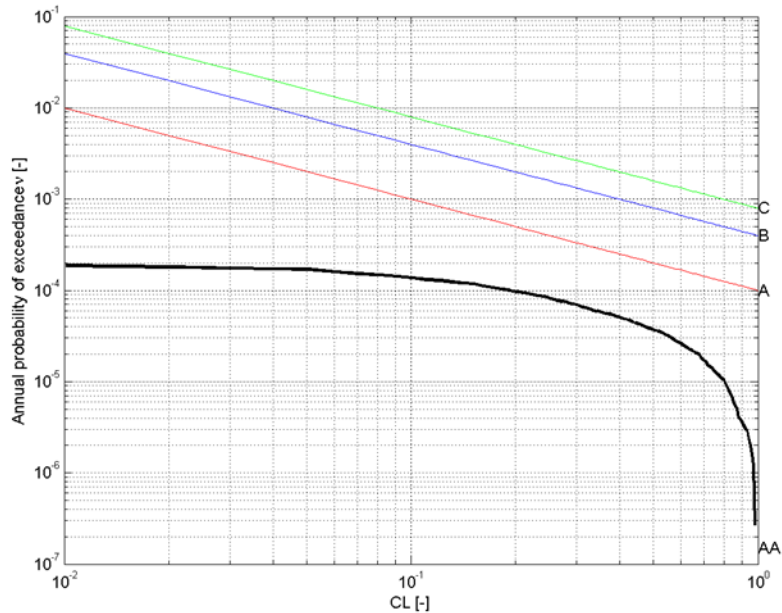


Figure 8. Exceedance frequencies for connectivity loss relative to (indicative) grading boundaries

7. Application to port infrastructures of Thessaloniki in Greece

This section outlines the application of the stress test methodology to the port of Thessaloniki, one of the most important ports in Southeast Europe and the largest transit-trade port in Greece. Ground shaking, liquefaction and tsunami hazards have been considered in the case study. Readers are referred to Pitilakis et al. (2017) for more details on this stress test.

7.1 Pre-Assessment phase

A GIS database for the examined port facilities, i.e. waterfront structures, cargo handling equipment, buildings (offices, sheds, warehouses etc.) and the electric power supply system has been developed. The Port subsoil conditions are characterized by soft alluvial deposits, sometimes susceptible to liquefaction. All necessary information to perform site specific ground response analyses were obtained by a comprehensive set of in-situ geotechnical tests (e.g. drillings, sampling, SPT and CPT tests), detailed laboratory tests and measurements, as well as geophysical surveys (cross-hole, down-hole, array microtremor measurements) at the port broader area. A topobathymetric model was also produced for the tsunami simulations, based on nautical and topographic maps and satellite images (Cotton et al. 2016; Selva et al. 2016).

The vulnerability of the port infrastructures to the given target hazards is assessed using site and case specific or generic fragility functions. New seismic fragility curves have been developed for typical quay walls and gantry cranes subjected to ground shaking based on dynamic numerical analyses. Analytical tsunami fragility curves as a function of inundation depth have been developed for representative typologies of RC buildings, warehouses and gantry cranes (Karafagka et al. 2016; Salzano et al. 2015). For simplicity reasons, the waterfront structures were

523 considered as non-vulnerable to tsunami forces. The electric power lines were also assumed as non-vulnerable for
524 the three hazards.

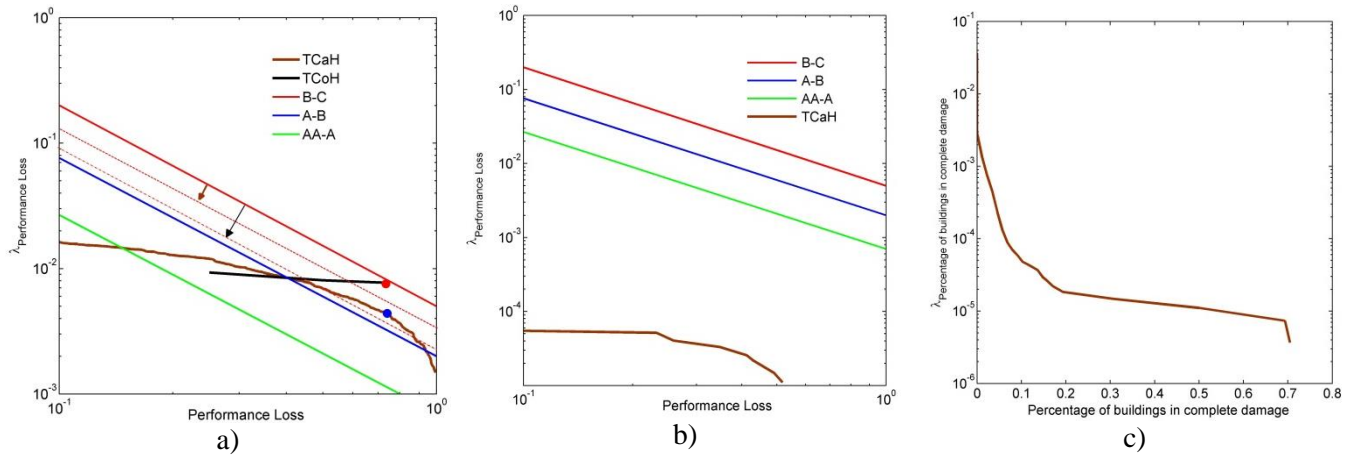
525 The stress test includes a component level risk based assessment of the key components (ST-L1) and a
526 probabilistic risk analysis at the system level (ST-L2). A complementary scenario-based system wide risk
527 assessment is also conducted associated to two earthquake return periods. Specific risk measures and acceptance
528 criteria have been defined related to the functionality of the port at system level and the structural losses at
529 component level. Since two terminals (container, bulk cargo) were assumed herein, the system performance is
530 measured through the total number of containers handled (loaded and unloaded) per day (TCoH), in Twenty-foot
531 Equivalent Units (TEU), and the total cargo handled (loaded and unloaded) per day (TCaH), in tones. Risk
532 measures related to structural and economic losses of the buildings were also set for the tsunami case and the
533 scenario-based assessment. Since no regulatory boundaries exist for the moment for port facilities, continuous
534 (Figure 9) and scalar boundaries (Table 9) were defined based on general judgment criteria for the probabilistic
535 and scenario-based system-wide risk assessment respectively.

536 **7.2 Assessment phase**

537 In the component level assessment, a risk-based assessment of each component is carried out for earthquake and
538 tsunami hazards to check whether the component passes or fails the minimum requirements for its performance.
539 The hazard function at the location of the component and the fragility function of the component are convolved in
540 risk integral in order to obtain the probability of exceedance of a designated limit state in a period of time. To
541 check whether or not the component is safe against collapse, the target probability was compared with the
542 corresponding probability of exceeding the ultimate damage state. A reference target probability of collapse equal
543 to $1 \cdot 10^{-5}$ has been pre-defined based on the existing practice.

544 In the system level assessment, a probabilistic risk analysis (PRA) is conducted separately for earthquake and
545 tsunami hazards considering specific interdependencies between network and components. The objective is to
546 evaluate the mean annual frequency (MAF) of events with the corresponding loss in the performance of the port
547 operations. The analysis was based on an object-oriented paradigm where the system is described through a set of
548 classes, characterized in terms of attributes and methods, interacting with each other (Franchin et al 2011; Kakderi
549 et al. 2014). A Monte Carlo simulation is carried out sampling events and corresponding damages for the given
550 hazards. The seismic hazard is based on the 2013 European Seismic Hazard Model - ESHM13 (Woessner et al
551 2015, Giardini et al 2013) and the modeling procedure described in Weatherill et al. (2014). The tsunami hazard
552 analysis was performed considering tsunamis generated by co-seismic sea floor displacements due to earthquakes
553 (e.g., Grezio et al. 2017; Davies et al. 2017; Lorito et al. 2015) and obtaining 253 representative scenarios based
554 on inundation simulation of the Thessaloniki area (Selva et al. 2016). The performance indicators (PIs) of the port
555 system for both the container and cargo terminal were evaluated for each simulation based on the damages and
556 corresponding functionality states of each component and considering the interdependencies between

557 components. The final computed PIs are normalized to the value referring to normal (non-seismic) conditions
 558 (P_{max}) assuming that all cranes are working at their full capacity 24 hours per day while the performance loss is
 559 defined as $1-PI/PI_{max}$.



560 **Figure 9.** MAF of exceedance curves for the port system PIs (TCoH, TCaH) in terms of normalized performance loss ($1-PI/PI_{max}$) for the seismic (a) and tsunami (b) hazard case and the buildings in collapse state for the tsunami case (c).
 561

562

563 For the seismic hazard case, Figure 9a shows the MAF of exceedance curves (“performance curve”) for the
 564 normalized performance loss in terms of TCoH and TCaH. The green, blue and red continuous lines correspond to
 565 the boundaries between risk grades AA (negligible), A (ALARP), B (possibly unjustifiable risk), and C
 566 (intolerable). For performance loss values below 40% TCaH yields higher values of exceedance frequency, while
 567 for performance loss over 40% TCoH yields higher values of exceedance frequency. For the tsunami hazard case,
 568 an example for one of the alternative models (i.e. the epistemic uncertainty is not considered here) is presented in
 569 Figure 9b. The container terminal is not expected to experience any loss (TCoH), while the loss in the cargo
 570 terminal (TCaH) is very low. This is due to the non-vulnerable condition of waterfront structures, the high
 571 damage thresholds for the cranes (i.e. inundation values that are not expected in the study area) and the distance of
 572 the electric power substations from the shoreline. The annual probabilities for buildings collapses are also low
 573 (Figure 9c). As an example 10% of the total buildings in the Port (~9 structures) will be completely damaged
 574 under tsunami forces with annual probability equal to $5 \cdot 10^{-5}$.

575 The scenario-based risk analysis (SBRA) is performed complementary to the classical PRA approach described
 576 previously, to quantify the potential impact of the local site response at the port area and to reduce the
 577 corresponding uncertainties. This type of effects may be of major importance in port areas, and by adopting
 578 specific scenarios is possible to model the site response more accurately than in standard PRA. Two different
 579 seismic scenarios were defined in collaboration with a pool of experts: the standard seismic design scenario and
 580 an extreme scenario corresponding to return periods of $T_m=475$ years and $T_m=4975$ years respectively. For the
 581 475 years scenario a set of 15 accelerograms was selected to fit the target spectrum defined based on the

582 disaggregation of the probabilistic seismic hazard analysis results (SRM-LIFE 2007; Papaioannou 2004) and the
583 median plus 0.5 standard deviation of Akkar and Bommer (2010) spectrum (Pitilakis et al. 2019). For the 4975
584 years scenario the selection of ground motion requires special attention considering that it might be an extreme
585 event that has not been recorded yet. Thus, two different approaches were considered: 4975 years scenario I and II
586 (Pitilakis et al. 2019). In particular, 10 synthetic accelerograms were computed to fit the target spectrum (median
587 plus one standard deviation Akkar and Bommer (2010) spectrum) (4975 years scenario I) and broadband ground
588 motions were generated (Smerzini et al. 2016) using 3D physics-based “source-to-site” numerical simulations
589 (4975 years scenario II). 1D equivalent-linear (EQL) and nonlinear (NL) site response analyses including also the
590 potential for liquefaction are carried out. It is observed that the EQL approach is associated with higher number of
591 non-functional components for all considered seismic scenarios whereas for the NL approach non-functional
592 components are present only for the 4975 years scenario I (Table 9). This is due among other factors to the
593 significantly higher PGA values calculated using the EQL approximation, which lead to higher damage
594 probabilities and consequently higher performance loss. Thus, even though the vulnerability using the NL
595 approach is assessed considering both ground shaking and liquefaction hazards, the estimated combined
596 exceedance probabilities and the corresponding performance loss are still lower compared to the ones predicted
597 by the EQL approach (Pitilakis et al. 2019).. As also evidenced by the estimated functionality state of each
598 component, the port system is non-functional both in terms of TCaH and TCoH for the 4975 years scenario I. A
599 100% and 67% performance loss is estimated for the TCoH and TCaH respectively when considering the EQL
600 approach for the 475 and 4975 years II scenarios, while the port is fully functional when considering the NL
601 approach both in terms of TCaH and TCoH for the latter scenarios.

602
603 **Table 9.** Estimated normalized performance loss of the port system for TCaH and TCoH and comparison with risk
604 acceptance criteria for the scenario-based assessment

Scenario	Analysis type	Performance loss (1-PI/PI _{max})		Risk acceptance criteria			Stress test outcome	
		TCaH	TCoH	AA-A	A-B	B-C	TCaH	TCoH
475 years	EQL	0.67	1.00	0.10	0.30	0.50	Fail	Fail
	NL	0.00	0.00				Pass	Pass
4975 years I	EQL	1.00	1.00	0.30	0.50	0.70	Fail	Fail
	NL	1.00	1.00				Fail	Fail
4975 years II	EQL	0.67	1.00				Partly pass	Fail
	NL	0.00	0.00				Pass	Pass

606 7.3 Decision phase

607 With reference to seismic hazard for both bulk cargo and container terminals, the port obtains grade B, meaning
608 that the risk is possibly unjustifiable and the CI partly passes this evaluation. The basis for redefinition of risk

609 objectives in the next stress test evaluation is the characteristic point of risk, which is defined as the point
610 associated with the greatest risk above the ALARP region. The CI receives grade AA (negligible risk), and as
611 expected in this example application, passes the stress test for the tsunami hazard. Based on the proposed grading
612 system, for the case which the port obtains grade B and partly passes the stress test, the B-C boundary in the next
613 stress test is reduced (i.e. B-C: 53% performance loss) while the other boundaries remain unchanged (Figure 9a).
614 The scenario-based assessment showed that the CI may pass, partly pass or fail for the specific evaluation of the
615 stress test (receiving grades AA, B and C respectively) depending on the selected seismic scenario, the analysis
616 approach and the considered risk metric. This level of analysis is complementary to the PRA and shows that a
617 detailed modelling of local site effects is of major importance for the outcome of the stress test. It is also worth
618 noting that the risk objectives and the time between successive stress tests should be defined by the CI authority
619 and regulator. Since regulatory requirements do not yet exist for the port infrastructures, the boundaries need to
620 rely on judgments.

621

622 **7.4 Report phase**

623 For the selected target probabilities of collapse, all port components are deemed as unsafe towards seismic
624 hazards at the component level assessment (ST-L1), while only few cranes are characterized as safe against
625 exceedance of the collapse limit state for the tsunami hazard. These results cannot be judged unconditional to the
626 fact that subjective boundaries relying on expert judgments are used, since regulatory requirements for port
627 infrastructures do not yet exist.

628 For ST-L2, and for the seismic case, several electric power distribution substations present high failure risk and
629 contribute to the performance loss of the port due to loss of power supply to the cranes. It is recommended to
630 investigate further the response of the substations under seismic shaking and consider potential upgrade or/and
631 alternative power sources. The systemic tsunami risk connected to direct damages from waves results not
632 significant. This is primarily connected to the physical position of the port (with relatively low tsunami hazard)
633 and the low fragility of components to tsunami waves. However, the potential effects of debris collisions have not
634 been accounted for. Therefore, a careful check of preparedness against tsunami should be suggested, ranging from
635 the connection to efficient tsunami warning systems as well as the definition of actions to secure ships and port
636 equipment.

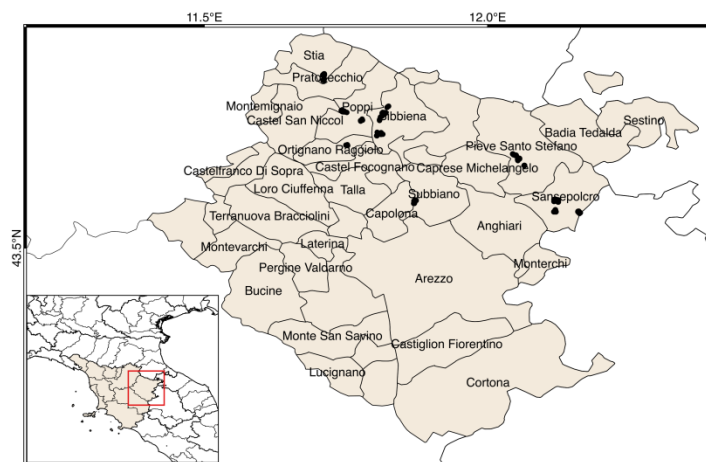
637 For the scenario-based assessment the estimated losses are significantly dependent on the analysis approach. In
638 particular, the EQL approach is associated with higher losses even for the design scenario (475 years), while for
639 the NL approach the losses to the cranes, waterfronts and electric power substations are expected solely for the
640 4975 scenario I. Therefore, the impact of local site effects on the stress test outcome is very important and should
641 be considered in the PRA through advanced seismic site response analysis.

642 **The risk mitigation and resilience planning for the port infrastructure include preventive, e.g.**
643 **early warning systems for earthquakes and tsunami, retrofitting of high-risk facilities,**
644 **improvement of foundation soil, updating of contingency plans and training exercises, and**
645 **reactive measures, e.g. efficient emergency and restoration plans, back-up capabilities for such as**
646 **use of mobile cranes or diesel generators for power supply. In this context, Galbusera et al. (2018)**
647 **performed a resilience analysis for the port infrastructures of Thessaloniki, considering the**
648 **fragility and importance of each component, the interdependencies, the recovery priorities and the**
649 **buffering capabilities for given seismic scenarios. Stress testing can further benefit the resilience**
650 **planning, while the effective communication between the key actors (e.g. port authority, operators,**
651 **experts) is essential.****8. Application to industrial district in Italy**

652 The performance and consequences assessment of an industrial building stock in Northern Italy, and more
653 specifically in the region of Tuscany, is presented in this case study. Only seismic hazard has been considered, as
654 it is the predominant hazard to which the industrial building stock in Tuscany is exposed. The limited budget for a
655 stress test of an industrial district (given that these facilities do not serve the same critical functions as other
656 infrastructure considered herein) has conditioned the level of detail and complexity of the stress test.
657 Nevertheless, the simplicity of the case study allows the full probabilistic risk assessment and disaggregation
658 methodology to be fully demonstrated. Readers are referred to Rodrigues et al. (2017) for more details on this
659 stress test.

660 **8.1 Pre-Assessment phase**

661 The exposure data of the industrial infrastructure in Tuscany have been provided by the Seismic Section of the
662 Tuscany Region. The details related to 300 industrial buildings in the province of Arezzo were used for the case
663 study, which included the geographical location (represented by a pair of coordinates), year of construction, floor
664 area, structural type, non-structural elements, and other data useful for identifying the value of contents, type of
665 business, and geographical extent of the facility's customer base (Figure 10).



666 **Figure 10.** Location of the 300 industrial facilities in the province of Arezzo. Due to the close proximity of some of the
667 buildings, each point that is shown on this map could represent up to 20 buildings
668

669
670 The majority of reinforced concrete precast industrial buildings in the Tuscany region can be categorized into
671 three classes as a function of the design code level (pre-code or low-code, depending on whether the buildings
672 were constructed before or after 1996), type of structure (type 1 buildings with long saddle roof beams, and type 2
673 with shorter rectangular beams and larger distances between the portals) and type of cladding (vertical precast
674 panels (V), horizontal panels (H) and concrete masonry infills (M)). Once the building subclass has been assigned
675 to each building in the exposure model, it is then necessary to add the value of the structural components, non-
676 structural components, contents and business interruption (in terms of revenue per day). Typical construction
677 costs for an industrial facility are used to assign the value of the structural and non-structural elements, estimated
678 using the mean market prices of industrial/typical warehouses as a function of their location within so-called OMI
679 zones “*Osservatorio del Mercato Immobiliare*” (Italian Revenue Agency 2016). The industrial sector in the
680 Tuscany region is dominated by mining due to the abundance of underground resources, but also textiles
681 industries, chemicals/pharmaceuticals, metalworking and steel, glass and ceramics, clothing and
682 printing/publishing sectors have a strong presence in the region. Specific data on the contents of each industrial
683 building was not available in the current database, and so the contents categories that are commonly damaged in
684 Italian industrial buildings have been considered to be present in all buildings (until more reliable information on
685 the contents of each building is available): i.e. fragile stock and supplies on shelves, computer equipment,
686 industrial racks and movable manufacturing equipment. The cost of the contents has been estimated according to
687 FEMA (2012), where it states that the value of the contents for the type of facilities considered herein can be
688 assumed to be 44% of the total value of the construction. Finally, business interruption costs have been estimated
689 using the HAZUS methodology (FEMA 2003).

690 Structural and non-structural fragility functions were derived using the analytical framework as described in Babič
691 and Dolšek (2016). The contents fragility functions were derived using a simplification of the procedure in ATC-
692 58 (ATC 2012), as proposed by Porter et al. (2012). Business interruption is defined herein as the time needed to
693 repair building damage, and so median downtimes have been estimated for each damage state in the structural
694 fragility functions. The downtime is currently only related to the structural damage as it is assumed that any non-
695 structural damage can be addressed in parallel during the time required to recover from structural damage.

696 For the hazard model, the three source models (area sources, fault sources and distributed seismicity) of the 2013
697 European Seismic Hazard Model, ESHM13 (Woessner et al. 2015) were used together with a ground-motion
698 prediction tree (GMPE) logic tree described in Rodrigues et al. (2017).

699 The stress test includes a component level risk based assessment of the key components, i.e. the industrial
700 buildings, (ST-L1) and a probabilistic risk analysis to assess the economic losses at the system level, combining
701 structural, non-structural, and contents damage as well as business interruption (ST-L2).

702 **8.2 Assessment and Decision Phase**

703 The annual probability of collapse for the component-based assessment only considers the structural components
704 of the facilities (as these are the only components that need to be legally considered in design). This risk-based
705 component level assessment has been undertaken for the 300 industrial facilities in Arezzo (see Figure 10) using
706 hazard curves (i.e. PGA versus annual probability of exceedance) estimated with the OpenQuake-engine (Pagani
707 et al. 2014) using the ESHM13 (Woessner et al. 2015), amplified considering topography-based V_{s30} estimates
708 (USGS 2016), together with the complete damage structural fragility functions for each sub-class of structure
709 (Babič and Dolšek 2016). According to the proposed grading system none of the structures has an annual
710 probability of collapse below $1 \cdot 10^{-5}$ (the specified A-B boundary), which means that all facilities are classified as
711 “partly pass” or “fail”. More specifically, 260 facilities are assigned grade B (partly pass) and the others 40
712 facilities are assigned grade C (and thus fail), as they had an annual probability of collapse below $2.0 \cdot 10^{-4}$ (the
713 specified B-C boundary).

714 For the system level assessment (where the seismic damage to a whole industrial district is estimated), economic
715 loss-based measures and objectives have been used due to the large losses that were experienced in Italy
716 following the Emilia-Romagna earthquakes (see Krausmann et al. 2014). The economic loss has been estimated
717 considering the losses due to structural damage, non-structural damage, contents damage and associated direct
718 business interruption (due to downtime). Specific objectives for these risk metrics have not yet been defined by
719 stakeholders in the industrial facilities, and thus hypothetical values have been considered herein for illustrative
720 purposes of the methodology. The threshold for the total AAL at the A-B boundary was defined as 0.05% of the
721 total exposure value, and 0.10% for the B-C boundary. For the second objective, the loss due to business
722 interruption at a mean annual rate of 10^{-4} (i.e. 1 in 10,000 years) should not be higher than 7 times the daily
723 business interruption exposure (i.e. 10 million €) for the A-B boundary, and not greater than 30 days for the B-C
724 boundary (42 million €).

725 In order to calculate probabilistic seismic risk for the spatially distributed portfolio of assets in Arezzo, the
726 Probabilistic Event-Based Risk (PEBR) calculator from the OpenQuake-engine (Silva et al. 2014) has been
727 employed. This calculator generates loss exceedance curves and risk maps for various return periods based on
728 probabilistic seismic hazard, within a Monte Carlo event-based approach.

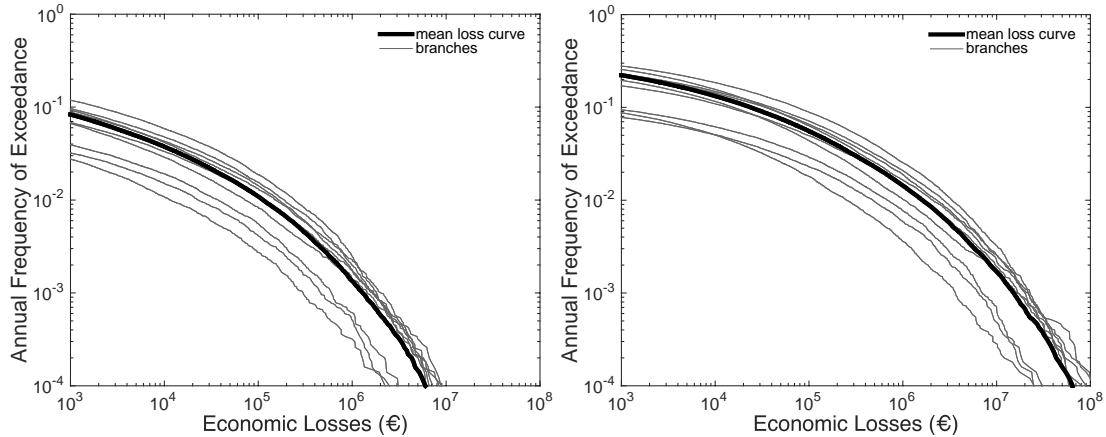
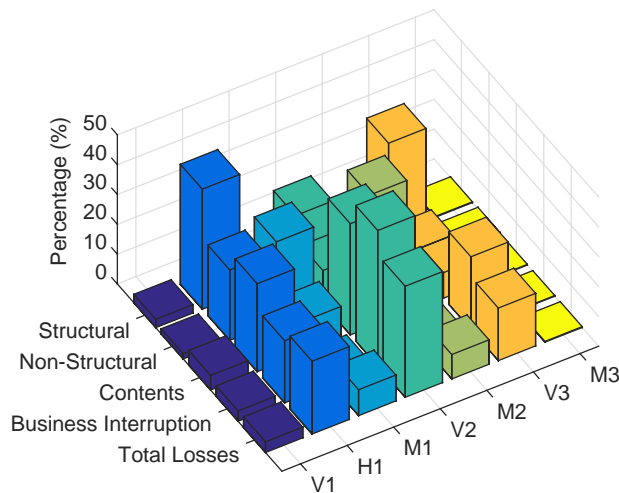


Figure 11. Loss exceedance curves for (left) structural and (right) business interruption losses in Arezzo

729
730

731 The average annual losses (AAL) have also been calculated from the loss exceedance curves in Figure 11 and
 732 these results show that the largest component of loss is given by business interruption. The results also indicate
 733 that the A-B system level assessment objective is not met (as the total AAL percentage is 0.052%), but the B-C
 734 level is instead met. Hence the grading would be B (partly pass) for this objective. The business interruption loss
 735 at a mean annual rate of exceedance of 10^{-4} is 64 million € (which can be translated as an average of 45 days of
 736 business interruption), and so the grading would be C (fail) for this objective.

737 In order to develop a potential risk reduction strategy, it is relevant to better understand which sub-classes of the
 738 industrial facilities are contributing most for the average annual losses, and to identify the type of hazard events
 739 that contribute to different loss levels. The disaggregation of the average annual loss, in terms of the critical
 740 components for each loss, are given in Figure 12. The sub-typologies that contribute most to the total average
 741 annual losses are V2 (i.e. pre-code type 2 portal frame with vertical cladding), H1 (i.e. pre-code type 1 portal
 742 frame with horizontal cladding) and V3 (i.e. low-code type 2 portal frame with vertical cladding).



743
744

Figure 12. Disaggregation of AAL according to building sub-class for each component of loss

745 **8.3 Report Phase**

746 Although each industrial building has not been assessed individually in detail according to current
747 Italian/European design requirements for single buildings, the results of the component-based assessment indicate
748 that a significant percentage would not meet current design requirements. The final overall outcome of the stress
749 test is driven by the system-level test and is deemed to be C (intolerable/fail), and thus this should stimulate
750 stakeholders to upgrade the existing industrial districts such that they will improve their grading in the following
751 stress test cycle. The performance of these pre-cast buildings would be significantly improved by strengthening
752 the weak beam-column connections. Collaborative action from a large number of stakeholders, represented by the
753 owners of each industrial warehouse, is required to improve the grading of the stress test, and this should be
754 encouraged and enforced by the regulatory authorities.

755 However, it is noted that the outcomes of the stress test presented herein are highly influenced by the assumptions
756 made in developing the exposure model as well as the definition of the target objectives, which have been defined
757 herein by the authors rather than the relevant stakeholders. Hence, further comments on the outcome of the stress
758 test are not made in these conclusions and instead it is stressed that additional efforts are needed in the future to
759 work with the owners of the industrial facilities to collect reliable content and annual revenue data, and to identify
760 the most appropriate target objectives.

761 **9. Discussion - Conclusions**

762 An engineering risk-based methodology for conducting stress tests of critical non-nuclear infrastructures has been
763 applied to six CIs in Europe. Different stress test levels were selected according to the characteristics of the
764 particular CIs and the available resources. The objective was to demonstrate the efficiency of the methodology
765 and how the proposed framework can be specified and implemented with regard to different types of CIs, i.e.
766 single site, geographically extended, distributed multi-site, each one exposed to varying hazards. These case
767 studies can be used as a basis for similar types of CIs, while the proposed framework can be adjusted and
768 implemented to other sectors. However, risk measures and acceptance criteria may vary depending on the
769 peculiarities of each CI, even if of similar type. For example, in case of port facilities, a risk measure in terms of
770 economic loss could be an alternative, instead of the loss in terms of cargo or container handled that is used in the
771 present application. Inevitably, the heterogeneity of the different CIs justifies the reasonable assumptions and/or
772 simplifications made in some steps of the applications. In this context, the authors disavow a quantitative
773 interpretation of the results provided, as these applications were not, nor should they be, considered formal stress
774 tests in each particular CI. In Table 10, the key elements of the six case studies are summarised, i.e. CI data,
775 hazard data, risk measures, risk acceptance criteria (component, system), stress test level, risk acceptance check,
776 and risk mitigation guidelines.

777

778 *The Table is provided at the end of the document***Table 10.** Overview of the key elements of the six stress test case
779 studies
780

781 The stress test to the oil refinery of Milazzo showed that the earthquake impact is important for the atmospheric
782 storage tanks. The tsunami effect on the atmospheric storage vessels along the shore line is relatively negligible
783 in terms of cascading effects and increase of the overall risk on population. Neither an earthquake nor a tsunami
784 significantly increases the failure frequency of, and hence the risk imposed by, pressurized vessels. Despite this,
785 the risk remains largely dominated by the LPG tanks failures due to industrial-related causes, whereas the impact
786 of the natural hazards is limited. Mitigation measures include the enhancement of the emergency preparedness for
787 multiple fire scenarios and the structural upgrade of tanks.

788 The stress test to a large dam in Switzerland exposed to multi-hazard effects, considering earthquakes, floods,
789 internal erosion and electromechanical malfunctions in key systems, showed that the first of three risk objectives
790 concerning the dam-reservoir system and the probability of failures taking place was met. The second objective,
791 related to the expected losses downstream was not met, while the third one, defined on the basis of an F-N curve,
792 classified the risk as ALARP (as low as reasonably practicable). The most efficient mitigation measure is to
793 upgrade the bottom outlet of the dam to prevent all overtopping events. Also, the resilience of the dam-reservoir
794 is very much defined by the capacity to perform a successful and timely drawdown operation, therefore cascade
795 effects become important when the possibility of drawing down the reservoir is lost, and a substantial inflow
796 arrives. The mitigation measures for the downstream area include the reinforcement or relocation of the high-risk
797 buildings, the installation of early warning systems and the improvement of emergency planning, e.g. shelters,
798 escape routes.

799 The application to Baku-Tbilisi-Ceyhan pipeline that crosses strike-slip fault segments in the eastern Anatolia in
800 Turkey, indicated that two pipe-fault crossings are critical as their failure rates exceed the allowable rate. The risk
801 assessment showed that risk is classified possibly unjustifiable. The risk mitigation guidelines are focused at the
802 retrofitting of the pipelines at the critical crossings by changing the angle of the pipe-fault intersection.

803 The stress test to the Gasunie gas distribution network in Groningen, Netherlands, exposed to earthquake and
804 liquefaction effects, showed that soil liquefaction is the dominant failure mechanism. In particular, with respect to
805 components, the pipe sections pass the stress test, while stations pass the stress test only partially. With respect to
806 the systemic risk the stress test is passed. The safety and resilience of this CI will be improved by reassessing the
807 need for retrofitting of the critical pipe sections identified in this study. The stress test also revealed the need for
808 site-specific fragility functions for the stations and the need for further research into the liquefaction mechanisms
809 for the Groningen site conditions.

810 The stress test to the port infrastructures of Thessaloniki exposed to seismic, tsunami and liquefaction hazards
811 showed a variation in the outcomes depending on the type of analysis. Most of the port components do not pass

812 the safety test against collapse for both earthquake and tsunami hazards in the case of a component level
813 assessment. The systemic risk is possibly unjustifiable and negligible for the PRA of earthquake and tsunami
814 hazards respectively, meaning that the port partly passes or passes this evaluation of the stress test. The scenario-
815 based assessment showed the importance of the modelling approach of local site effects in the outcome of the
816 stress test. The proposed mitigation planning includes the potential upgrade of the electric power substations due
817 to their criticality for the port operations or/and the installation of alternative power sources. Moreover, the
818 resilience planning of the port should consider the fragility and importance of each component, interdependencies,
819 recovery priorities and buffering capabilities.

820 The stress test to an industrial district in Northern Italy, exposed to seismic hazard, concluded that the facilities
821 partly pass or fail to pass the component-based assessment. For the system level assessment, where economic
822 loss-based measures and objectives have been used, the industrial district partly passes or fails to pass the test
823 depending on the considered boundaries used as thresholds of loss due to business interruption. Risk mitigation
824 can be achieved on the basis of strengthening building sub-classes that contribute most to the total losses, in
825 particular the weak beam-column connections of pre-cast buildings.

826 In summary, standardized actions and results are foreseen in the proposed framework, which are defined based on
827 the level of stress testing and the level of detail that is applied. For example, if a low level is adopted leading to
828 lack of risk acceptance then a more advanced method should be used, while if a component fails the assessment
829 risk mitigation actions must be applied. In all six case studies the risk objectives boundaries have been set mainly
830 based on expert judgment. However, formulation of risk acceptance criteria is not a straightforward task. In
831 practice, setting objectives and establishing risk measures is difficult and strongly dependent on legal, socio-
832 economic and political contexts and they should be defined by the corresponding stakeholders. Nevertheless,
833 when needed, the results of the stress tests have the potential to stimulate stakeholders to take action to upgrade
834 the existing infrastructure aiming to improve their grading in the following stress test cycle toward improving the
835 resilience and preparedness of CIs. Lessons learned through the six applications is the need for improvement of
836 existing assessment approaches considering the uncertainties in the quantification of hazard, vulnerability and
837 loss estimates as well as the need for site-specific fragility models. An important issue is also the collaborative
838 action and effective communication of the key actors, i.e. stakeholders, experts, owners and operators of the CIs
839 and regulatory authorities.

840

841 **Acknowledgements**

842 The work presented in this paper was conducted within the project “*STREST: Harmonized approach to stress*
843 *tests for civil infrastructures against natural hazards*” funded by the European Community’s Seventh Framework
844 Programme under grant agreement no. 603389. The authors gratefully acknowledge this funding. The authors

845 acknowledge the contributions of the Work Package leaders, Mr Peter Zwicky, Prof Fabrice Cotton, Prof Iunio
846 Iervolino, Prof Bozidar Stojadinovic, Dr Fabio Taucer as well as Dr Simona Esposito, Prof Matjaž Dolšek and Dr
847 George Tsionis. The methods, results, opinions, findings and conclusions presented in this paper are those of the
848 authors and do not necessarily reflect the views of the European Commission or the owners and stakeholders of
849 the studied CIs.

850 **References**

- 851 Akkar S, Sandikkaya MA, Bommer JJ (2014a) Empirical ground-motion models for point-and extended-source
852 crustal earthquake scenarios in Europe and the Middle East. *Bulletin of Earthquake Engineering* 12(1):359–
853 387
- 854 Akkar S, Sandikkaya MA, Bommer JJ (2014b) Erratum to: Empirical ground-motion models for point- and
855 extended-source crustal earthquake scenarios in Europe and the Middle East. *Bulletin of Earthquake*
856 *Engineering* 12(1):389–390
- 857 American Lifelines Alliance (ALA) (2001). *Seismic Fragility Formulations for Water Systems, Part 1–Guideline*,
858 <http://www.americanlifelinesalliance.org>
- 859 ATC - Applied Technology Council (2012) *ATC-58: Guidelines for Seismic Performance Assessment of*
860 *Buildings, 100% Draft*. Redwood City, CA
- 861 Babič A, Dolšek M (2016) Seismic fragility functions of industrial precast building classes. *Engineering*
862 *Structures* 118: 357-370
- 863 Basco A, Salzano E (2016) The vulnerability of industrial equipment to tsunamis. *Journal of Loss Prevention in the*
864 *Process Industries* (in press), DOI: 10.1016/j.jlp.2016.11.009
- 865 Bommer JJ (2013) *Proposals for New GMPEs for the Prediction of PGA and PGV in the Groningen Gas Field*,
866 *NAM internal note, 37pp*
- 867 Chang SE (2000) *Disasters and transport systems: Loss, recovery, and competition at the Port of Kobe after the*
868 *1995 earthquake*. *J Transp Geogr* 8(1): 53–65
- 869 Cheng Y and Akkar S (2017) Probabilistic permanent fault displacement hazard via Monte Carlo simulation and
870 its consideration for the probabilistic risk assessment of buried continuous steel pipelines. *Earthquake*
871 *Engineering and Structural Dynamics* 46 (4), 605-620
- 872 Cotton F et al. (2016) *Deliverable 3.7: Multi-hazard assessment of low-probability hazard and LP-HC events for*
873 *six application areas. STREST project: Harmonized approach to stress tests for critical infrastructures against*
874 *natural hazards*, www.strest-eu.org
- 875 CPR 18E (1999) *Guidelines for quantitative risk assessment*. Committee for the Prevention of Disasters (CPR)
- 876 Davies G, Griffin J, Lovholt F, Glimsdal S, Harbitz C, Thio HK, Lorito S, Basili R, Selva J, Geist E, Baptista MA
877 (2017) *A global probabilistic tsunami hazard assessment from earthquake sources*, in *Tsunamis: Geology*,

878 Hazards and Risks (Scourse EM, Chapman NA, Tappin DR & Wallis SR Eds), Geological Society, London,
879 Special Publications, 456, <https://doi.org/10.1144/SP456.5>

880 Dost B, Caccavale M, Van Eck T, Kraaijpoel D (2013) Report on the expected PGV and PGA values for induced
881 earthquakes in the Groningen area, KNMI report, 26pp.
882 (http://bibliotheek.knmi.nl/knmipubDIV/Report_on_the_expected_PGV_and_PGA_values_for_induced_earth
883 [quakes.pdf](http://bibliotheek.knmi.nl/knmipubDIV/Report_on_the_expected_PGV_and_PGA_values_for_induced_earth))

884 EC (2012) Directive 2012/18/EU of the European Parliament and of the Council of 4 July 2012 on the control of
885 major-accident hazards involving dangerous substances, amending and subsequently repealing Council
886 Directive 96/82/EC. Off J Eur Union, pp. 1-37

887 EMDAT (2019) OFDA/CRED International disaster database, Université Catholique de Louvain, Brussels,
888 Belgium, <https://www.emdat.be/>

889 ENSREG (2012) Stress tests performed on European nuclear power plants. Peer Review Report. European
890 Nuclear Safety Regulators Group, available online: <http://www.ensreg.eu/node/407>

891 Eidinger JM, Avila EA (1999) Guidelines for the seismic evaluation and upgrade of water transmission facilities
892 (Vol. 15). ASCE Publications

893 Esposito S, Iervolino I, d'Onofrio A, Santo A, Franchin P, Cavalieri F (2015) Simulation-based seismic risk
894 assessment of a gas distribution network. Computer-Aided Civil and Infrastructure Engineering. DOI:
895 10.1111/mice.12105

896 Esposito S, Stojadinovic B, Babič A, Dolšek M, Iqbal S, Selva J, Broccardo M, Mignan A, Giardini D (2019) A
897 risk-based multi-level methodology to stress test critical non-nuclear infrastructure systems, Journal of
898 Infrastructure Systems (accepted).

899 Esposito S, Stojadinovic B, Mignan A, Dolšek M, Babič A, Selva J, Iqbal S, Cotton F, Iervolino I (2016)
900 Reference Report RR4: Guidelines for stress-test design for non-nuclear critical infrastructures and systems:
901 Methodology. STREST EC/FP7 project: Harmonized approach to stress tests for critical infrastructures against
902 natural hazards, www.strest-eu.org

903 FEMA (2003) Multi-hazard Loss Estimation Methodology, Earthquake Model, HAZUS. Federal Emergency
904 Management Agency and National Institute of Buildings Sciences, Washington DC

905 FEMA (2012) FEMA E-74: Reducing the risks of nonstructural earthquake damage – a practical guide, Report by
906 Federal Emergency Management Agency

907 Franchin P, Cavalieri F, Pinto PE, Lupoi A, Vanzi I, Gehl P, Kazai B, Weatherill G, Esposito S, Kakderi K (2011)
908 General methodology for systemic seismic vulnerability assessment. Deliverable 2.1 SYNER-G EC/FP7
909 project, <http://www.vce.at/SYNER-G/>

910 Galbusera L, Giannopoulos G, Argyroudis S, Kakderi K (2018). A Boolean Networks approach to modeling and
911 resilience analysis of interdependent critical infrastructures. *Computer-Aided Civil and Infrastructure*
912 *Engineering* 33(12): 1041-1055.

913 Giannopoulos G, Filippini R, Schimmer M (2012) Risk assessment methodologies for critical infrastructure
914 protection. Part I: A state of the art. Publications Office of the European Union, Luxembourg. doi:
915 10.2788/22260

916 Giardini D. et al. (2013) Seismic Hazard Harmonization in Europe (SHARE). Online Data Resource,
917 <http://portal.share-eu.org:8080/jetspeed/portal/>, doi: 10.12686/SED-00000001-SHARE

918 Grezio A, Babeyko A, Baptista MA, Behrens J, Costa A, Davies G, Geist EL, Glimsdal S, González FI, Griffin J,
919 Harbitz CB, LeVeque RJ, Lorito S, Løvholt F, Omira R, Mueller C, Paris R, Parsons T, Polet J, Power W,
920 Selva J, Sørensen MB, Thio HK (2017) Probabilistic Tsunami Hazard Analysis (PTHA): multiple sources and
921 global applications, *Reviews of Geophysics* 55: 1158-1198, DOI: 10.1002/2017RG000579

922 Grimaz S (2014) Can earthquakes trigger serious industrial accidents in Italy? Some considerations following the
923 experiences of 2009 L'Aquila (Italy) and 2012 Emilia (Italy) earthquakes. *Bollettino di Geofisica Teorica ed*
924 *Applicata* 55(1): 227-237. doi: 10.4430/bgta0116

925 Gunn R, Balissat M, Manso P, et al. (eds) (2016) Proceedings of the 13th International Benchmark Workshop on
926 Numerical Analysis of Dams. In: ICOLD Proceedings. Swiss Committee on Dams, Lausanne, Switzerland.

927 Gutenberg B, Richter CF, (1956). Magnitude and Energy of Earthquakes. *Annali di Geofisica* 9: 1–15. Helm P
928 (1996) Integrated Risk Management for Natural and Technological Disasters. *Tephra*. 15(1): 4-13.

929 Honegger DG, Wijewickreme D (2013) Seismic risk assessment for oil and gas pipelines. In *Handbook of*
930 *Seismic Risk Analysis and Management of Civil Infrastructure Systems* pp.682-715. Elsevier
931 <http://www.nexus.globalquakemodel.org/gem-vulnerability/posts/draft-content-vulnerability-guidelines>

932 Idriss IM, Boulanger RW, 2008. Soil Liquefaction during earthquake, EERI monograph MNO-12 on earthquake
933 engineering. Earthquake Engineering Research Institute, Oakland (CA), USA

934 Jonkman SN, Van Gelder PHAJM, Vrijling JK (2003) An overview of quantitative risk measures for loss of life
935 and economic damage. *Journal of Hazardous Materials* 99(1):1-30

936 Kakderi K, Selva J, Pitilakis K (2014) Application in the Harbor of Thessaloniki, in: K. Pitilakis et al. (eds).
937 Systemic seismic vulnerability and risk assessment of complex urban, utility, lifeline systems and critical
938 facilities. *Methodology and applications*, Springer Science+Business Media, Dordrecht, doi: 10.1007/978-94-
939 017-8835-9_12

940 Karafagka S, Fotopoulou S, Pitilakis K (2016) Tsunami fragility curves for seaport structures, In the 1st
941 International Conference on Natural Hazards & Infrastructure, Chania, Greece, June 28-30

942 Krausmann E, Cozzani V, Salzano E, Renni E (2011) Industrial accidents triggered by natural hazards: an
943 emerging risk issue. *Natural Hazards and Earth System Sciences* 11:921–929

944 Krausmann E, Cruz AM (2013) Impact of the 11 March 2011, Great East Japan earthquake and tsunami on the
945 chemical industry. *Nat Hazards* 67(2): 811–828. doi: 10.1007/s11069-013-0607-0

946 Krausmann E, Piccinelli R, Ay BÖ, Crowley H, Uckan E, Erdik M, Lanzano G, Salzano E, Iervolino I, Esposito
947 S, Pistolas A, Kakderi K, Pitilakis D, Pitilakis K, Steenbergen R (2014) Deliverable D2.3: Report on lessons
948 learned from recent catastrophic events. STREST EC/FP7 project: Harmonized approach to stress tests for
949 critical infrastructures against natural hazards, www.strest-eu.org

950 Krausmann E, Cruz AM, Salzano E (2016). *Natech Risk Assessment and Management - Reducing the Risk of*
951 *Natural-Hazard Impact on Hazardous Installations*, Elsevier, 1st Ed., ISBN-10: 0128038071, 268

952 Kutkov V.A, Tkachenko V.V. (2017). Fukushima Daiichi accident as a stress test for the national system for the
953 protection of the public in event of severe accident at NPP. *Nuclear Energy and Technology* 3(1):38-42.

954 Lorito S, Selva J, Basili R, Romano F, Tiberti MM, Piatanesi A (2015) Probabilistic hazard for seismically-
955 induced tsunamis: accuracy and feasibility of inundation maps, *Geophys J Int* 200(1):574-588

956 Mignan A, Wiemer S, Giardini D (2014) The quantification of low-probability–high-consequences events: part I.
957 A generic multi-risk approach. *Nat Hazards* 1–24. doi: 10.1007/s11069-014-1178-4

958 Mignan A, Danciu L, Giardini D (2015) Reassessment of the Maximum Fault Rupture Length of Strike-Slip
959 Earthquakes and Inference on M_{max} in the Anatolian Peninsula, Turkey. *Seismol. Soc. Am.*, 86, 890-900, doi:
960 10.1785/0220140252

961 Mignan A, Danciu L, Giardini D (2016a) Considering large earthquake clustering in seismic risk analysis. *Nat.*
962 *Hazards*, doi: 10.1007/s11069-016-2549-9

963 Mignan A, Scolobig A, Sauron A (2016b) Using reasoned imagination to learn about cascading hazards: a pilot
964 study. *Disaster Prevention and Management*, 25, 329-344, doi: 10.1108/DPM-06-2015-0137

965 Miraglia S, Courage W, Meijers P (2015) Fragility functions for pipeline in liquefiable sand: a case study on the
966 Groningen gas-network. In Haukaas T (Ed.) *In the 12th International Conference on Applications of Statistics*
967 *and Probability in Civil Engineering (ICASP12)*, Vancouver, Canada, July 12-15

968 National Institute of Building Sciences, NIBS (2004) *Direct physical damage-general building stock. HAZUS-*
969 *MH Technical manual, Chapter 5*. Federal Emergency Management Agency, Washington, D.C.

970 Newmark NM, Rosenblueth E (1971) *Fundamentals of earthquake engineering*. Englewood Cliffs: Prentice-
971 Hall. Opdyke A, Javernick-Will A, Koschmann M (2017) Infrastructure hazard resilience trends: an analysis of
972 25 years of research. *Nat Hazards* 87(2): 773–789. doi:10.1007/s11069-017-2792-8

973 Pagani M, Monelli D, Weatherill G, Danciu L, Crowley H, Silva V, Henshaw P, Butler L, Nastasi M, Panzeri L,
974 Simionato M and Vigano D (2014) OpenQuake Engine: An open hazard (and risk) software for the Global
975 Earthquake Model. *Seismological Research Letters*, 85(3): 692-702.

976 Pescaroli G, Alexander D (2016) Critical infrastructure, panarchies and the vulnerability paths of cascading
977 disasters. *Nat Hazards* 82(1): 175–192. doi: 10.1007/s11069-016-2186-3

978 Pitilakis K, Argyroudis S, Fotopoulou S, Karafagka S, Kakderi K, Selva J (2017). Application of new stress test
979 concepts for port infrastructures against natural hazards. The case of Thessaloniki port in Greece, Reliability
980 Engineering & System Safety 184:240-257.

981 Pitilakis K, Argyroudis S, Fotopoulou S, Karafagka S, Anastasiadis A, Pitilakis D, Raptakis D, Riga E, Tsinaris
982 A, Mara K, Selva J, Iqbal S, Volpe M, Tonini R, Romano F, Brizuela B, Piatanesi A, Basili R, Salzano E,
983 Basco A, Schleiss AJ, Matos JP, Akkar S, Cheng Y, Uckan E, Erdik M, Courage W, Reinders J, Crowley H,
984 Rodrigues D (2016). Deliverable D6.1: Integrated report detailing analyses, results and proposed hierarchical
985 set of stress tests for the six CIs. STREST EC/FP7 project: Harmonized approach to stress tests for critical
986 infrastructures against natural hazards, www.strest-eu.org

987 Porter K, Cho I, Farokhnia K (2012) Contents seismic vulnerability estimation guidelines. Global Vulnerability
988 Consortium

989 Renzi E, Basco A, Busini V, Cozzani V, Krausmann E, Rota R, Salzano E (2010). Awareness and mitigation
990 of NaTech accidents: Toward a methodology for risk assessment. Chemical Engineering Transactions 19:383-
991 389

992 Reuters (2010) Flash floods inundate central Europe, [http://www.reuters.com/article/2010/08/08/us-europe-](http://www.reuters.com/article/2010/08/08/us-europe-floods-idUSTRE67617F20100808)
993 [floods-idUSTRE67617F20100808](http://www.reuters.com/article/2010/08/08/us-europe-floods-idUSTRE67617F20100808)

994 Rodrigues D, Crowley H and Silva V (2017) Earthquake loss assessment of precast RC industrial structures in
995 Tuscany (Italy), Bulletin of Earthquake Engineering 16(2), DOI: 10.1007/s10518-017-0195-6

996 Salzano E, Basco A, Busini V, Cozzani V, Renzi E, Rota R (2013) Public Awareness Promoting New or
997 Emerging Risk: Industrial Accidents Triggered by Natural Hazards. Journal of Risk Research 16:469-485

998 Salzano E, Basco A, Karafagka S, Fotopoulou S, Pitilakis K, Anastasiadis A, Matos JP, Schleiss AJ (2015).
999 Deliverable D4.1: Guidelines for performance and consequences assessment of single-site, high-risk, non-
1000 nuclear critical infrastructures exposed to multiple natural hazards. STREST EC/FP7 project: Harmonized
1001 approach to stress tests for critical infrastructures against natural hazards, www.strest-eu.org

1002 Selva J, Iqbal S, Taroni M, Marzocchi W, Cotton F, Courage W, Abspoel-Bukman L, Miraglia S, Mignan A,
1003 Pitilakis K, Argyroudis S, Kakderi K, Pitilakis D, Tsiniadis G, Smerzini C (2015) Deliverable D3.1: Report on
1004 the effects of epistemic uncertainties on the definition of LP-HC events. STREST EC/FP7 project:
1005 Harmonized approach to stress tests for critical infrastructures against natural hazards, www.strest-eu.org

1006 Selva J, Tonini R, Romano F, Volpe M, Brizuela B, Piatanesi A, Basili R, Lorito S (2016) From regional to site
1007 specific SPTHA through inundation simulations: a case study for three test sites in Central Mediterranean.
1008 EGU General Assembly, Vienna, Austria, 17-22 April, Abstract #EGU2016-16988

1009 Silva V, Crowley H, Pagani M, Pinho R (2014) Development of the OpenQuake engine, the Global Earthquake
1010 Model's open-source software for seismic risk assessment. Natural Hazards, 72(3):1409-1427

1011 Smerzini C, Pitilakis K, Hasmemi K (2016) Evaluation of earthquake ground motion and site effects in the
1012 Thessaloniki urban area by 3D finite-fault numerical simulations. *B Earthq Eng*, 15(3):787–812

1013 Theocharidou M, Giannopoulos G (2015) Risk assessment methodologies for critical infrastructure protection.
1014 Part II: A new approach. Publications Office of the European Union, Luxembourg. doi: 10.2788/621843

1015 USGS (2016) Earthquake hazards program (Predefined Vs30 Mapping). Available at URL:
1016 <http://earthquake.usgs.gov/hazards/apps/vs30/predefined.php>

1017 Weatherill G, Esposito S, Iervolino I, Franchin P, Cavalieri F (2014) Framework for seismic hazard analysis of
1018 spatially distributed systems, in: K. Pitilakis et al. (eds). *Systemic seismic vulnerability and risk assessment of*
1019 *complex urban, utility, lifeline systems and critical facilities. Methodology and applications*, Springer
1020 Science+Business Media, Dordrecht, doi: 10.1007/978-94-017-8835-9_3

1021 WINN_TA-NAM (2016). Technical Addendum to the Winningsplan 2016. NAM, April 1st (in Dutch)

1022 Woessner J, Danciu L, Giardini D, Crowley H, Cotton F, Grunthal G, Valensise G, Arvidsson R, Basili R,
1023 Demircioglu M, Hiemar S, Meletti C, Musson R, Rovida A, Sesetyan K, Stucchi M (2015) The 2013 European
1024 Seismic Hazard Model-Key Components and Results. *Bulletin of Earthquake Engineering*, DOI
1025 10.1007/s10518-015-9795-1

1026 Zenz G, Goldgruber M (eds) (2013) *Proceedings of the 12th International Benchmark Workshop on Numerical*
1027 *Analysis of Dams*. ICOLD, Graz, Austria

1028

Table 10

	Oil refinery and petrochemical plant in Milazzo, Italy	Alpine earthfill dam, Switzerland	Baku-Tiblisi-Ceyhan pipeline, Turkey	Gasunie national gas storage and distribution network, Netherlands	Port infrastructure of Thessaloniki, Greece	Industrial district in the region of Tuscany, Italy
CI data						
Number of components	177 hydrocarbons storage tanks (gasoline, gasoil, crude oil, LPG)	conceptual dam-reservoir system: dam and foundation, spillways, bottom outlet, hydropower system and reservoir. downstream area: approx. 1000 buildings	1,800 km buried pipeline of crude oil	~1,000 km pipe network for gas transport; 11 M&R stations; 15 feeding points and 91 receiving points as end nodes	25 waterfront structures (WS); 35 cargo handling equipment (CE); 4 gantry cranes (GC); 85 building and storage facilities (BD); electric power lines (EL) and 17 distribution substations (ES)	300 buildings (structural elements)
Typology	steel storage tanks with variable capacities: 100 m ³ (fuel oil, gasoil, gasoline, kerosene) to 160 000 m ³ (crude oil) located in catch basins (bunds) with concrete surfaces. LPG: pressurised spheres	dam-reservoir system: custom typology; height: 100 m, reservoir capacity: 100 000 000 m ³ downstream area: buildings grouped according to the number of storeys	material: steel API XL Grade X65; diameter: 42 inches; thickness: 20.62mm; buried depth: 1.5m	main gas transmission pipes (4 to 8 MPa); diameters ranging from 114 mm to 1219 mm; M&R stations: predominately small masonry buildings	WS: concrete gravity block type quay walls, non-anchored components; CE: non-anchored components without backup power supply; GC: capacity 45 tons; EL: non-vulnerable; ES: low-voltage, with non-anchored components	pre-code or low-code reinforced concrete precast industrial buildings
Hazard data						
Hazard type	seismic (ground shaking and liquefaction), tsunami	seismic, flood, internal erosion, bottom outlet malfunction, and hydropower system malfunction	permanent fault displacement (PFD)	seismic (ground shaking and liquefaction)	seismic (ground shaking and liquefaction), tsunami	seismic
Model	probabilistic seismic hazard analysis (PSHA); seismic probabilistic tsunami hazard analysis (SPTHA)	seismic hazard maps of the Swiss Seismological service; extreme flood analyses; expert knowledge and historically observed malfunction frequencies	PFD at 5 fault crossings: scenario-based (2475 years); uncertainty in pipe-fault angle crossing	PSHA: Z1 model for Groningen area (Dost et al. 2013); modified GMPE (Bommer 2013)	PSHA: ESHM13 and Weatherill et al. (2014). SPTHA: 253 representative scenarios based on inundation simulation. seismic scenario-based: 475 years (EQL, NL), 4975 years (EQL, NL)	2013 European Seismic Hazard Model (ESHM13)
Risk measures						
Component	annual probability of release of content of hazardous materials (defined standard mass flow rate)	1) annual probability of failure and 2) annual probability of household loss	annual probability of loss of pressure integrity	annual failure probability	annual probability of collapse	annual probability of collapse
System	locational and individual risk (fatalities/year); societal risk (F/N curve)	obj1: uncontrolled release of the reservoir; obj2: probability of a household being collapsed or washed away (lost	N/A	connectivity loss (Esposito et al., 2016)	normalized loss of: total number of containers handled (loaded and unloaded) per day (TCoH); total cargo handled (loaded	obj1: average annual loss; obj2: mean annual rate of economic loss (due to structural damage, non-structural damage, contents

		volume/year)			and unloaded) per day (TCaH)	damage and direct business interruption)
Risk acceptance criteria						
Component	target probability of collapse of equipment with the instantaneous release of content less or equal to 1.0×10^{-8}	all the components comply to and slightly exceed regulatory requirements (assumption of a conceptual dam)	target probability of pipeline failure in 2475 years: 4.0×10^{-5} scenario-based: AA-A: 2-10, A-B: 10-50, B-C: 50-100 (% loss for 2475 years)	AA-A: 8.0×10^{-6} A-B: 6.0×10^{-5} B-C: 1.4×10^{-4} Pipes (km/year); M&R stations (object/year)	target probability of collapse: 1.0×10^{-5}	target probability of collapse: A-B: 1.0×10^{-5} B-C: 2.0×10^{-4}
System*	fatality rate as given by acceptability parameters either for the locational risk (1.0×10^{-4} f/year for workers, 1.0×10^{-6} f/year for population) or for the societal curve ($F < 1.0 \times 10^{-3}/N^2$)	obj1: $p(\text{failure}) \leq 1.0 \times 10^{-5}$ obj2: AA-A: 7.5 m ³ /yr (~one household lost per 100 years), A-B: 75 m ³ /yr, B-C: 750 m ³ /yr (~one household lost per year)	N/A	AA-A: 1.0×10^{-4} , A-B: 4.0×10^{-4} , B-C: 8.0×10^{-4} , for annual probability of 100% loss (Esposito et al., 2016)	PSHA & SPTA: AA-A: 7.5×10^{-4} , A-B: 2.0×10^{-3} , B-C: 4.5×10^{-3} , for annual probability of 100% loss. scenario-based: AA-A: 10, A-B: 30, B-C: 50 (% loss for 475 years) AA-A: 30, A-B: 50, B-C: 70 (% loss for 4975 years)	obj1: A-B: 0.05%, B-C: 0.1% obj2: A-B: 10^{-4} for 10 Million Euro loss (7 days), B-C: 10^{-4} for 42 million Euro loss (30 days)
Stress test level	ST-L1a; ST-L2b; ST-L2d	ST-L2b/L2d; ST-L3c/L3d	ST-L1	ST-L1; ST-L2a	ST-L1; ST-L2b; ST-L2d/L3d	ST-L1; ST-L2a
Risk acceptance check (AA-A: pass, B: partly pass, C: fail)	ST-L1a, ST-L2b, ST-L2d: AA-C (earthquake), AA-C (tsunami)	ST-L2 (seismic): AA-A ST-L3 (all five hazards): AA-A	ST-L1: (hazard based assessment), fault crossings #2, #3 and #4 do not comply with the code requirements. ST-L1: (design based assessment), all five crossings comply with the code requirements. ST-L1: B (risk based assessment), fault crossings #3 and #4 do not comply with the target risk tolerance	ST-L1 (components): AA-B ST-L2a (system): AA-A (see Table 8)	ST-L1: C (seismic), AA-C (tsunami) ST-L2b: B (seismic), AA (tsunami) ST-L2d/L3d: AA, A, B, C (depending on the scenario and analysis type, see Table 9)	ST-L1: B (260 facilities), C (40 facilities) ST-L2a: B for obj1, C for obj2
Risk mitigation guidelines	reinforcing of tanks for earthquake and tsunami-induced structural damage and defining the emergency response in case of release of hazardous materials	invest on the resilience of the reservoir drawdown mechanism (bottom outlet)	upgrading of two critical fault crossing points by changing the orientation angles of pipes (after upgrading, the risk is classified as AA)	retrofitting pipe sections identified; site-specific fragility functions for the Gasunie-GTS stations	consider potential upgrade of substations or/and alternative power sources; measures to secure ships and port equipment	upgrade of building subclasses that contribute most to the total losses

* boundaries for system risk acceptance criteria were based on expert judgement